A stochastic behaviour model of a personal mobility under heterogeneous low-carbon traffic flow

Seunghyeon Lee[a,*], Ingon Ryu[b], Dong Ngoduy[c], Nam H. Hoang[c], Keechoo Choi[b]

[a] *Faculty of Engineering and IT, University of Technology Sydney, Sydney, Australia*
[b] *Department of Transportation Engineering, Ajou University, Suwon, South Korea*
[c] *Institute of Transport Studies, Monash University, Melbourne, Australia*

Abstract

The study proposes a mathematical framework to explain the stochastic behavioural patterns of personal mobility (PM) devices under low-carbon heterogeneous traffic conditions in shared lanes. We create a set of anticipation factors in a stochastic PM behaviour model to tackle sensitivities to both space headway and relative speed against intra- and inter-modes. The proposed behaviour model involves a deterministic and a stochastic force. In the deterministic force, the anticipation factors are used in an optimal velocity model and a full velocity difference model. In the stochastic force, the Langevin equation is used to capture PMs' stochastic characteristics against movements of other PMs, pedestrians, and bicycles, and the effect of lateral interactions. We carried out real-world circular experiments of mixed sustainable modes to verify the performance of the proposed models. Five models' performances are compared under four different traffic conditions, including bike-mixed, pedestrian-mixed, low-speed, and high-speed conditions. We confirmed that newly created anticipation factors play a significant role in all models under all conditions to partially influence the following PM devices' behaviour from the leading two different sustainable modes. The validation results illustrate the excellence of the proposed method. Consequently, behavioural uncertainty is well captured by the stochastic PM devices following models under all traffic conditions, although it requires more parameters than the deterministic PM behavioural models. The proposed method paves the way for the stochastic CF model's applicability to describe PM devices' behavioural dynamics under mixed traffic conditions using anticipation factors. Besides, it lays the foundation stone of PM devices' dynamics in a shared lane to construct effective regulations and safety standards.

Keywords: Stochastic behaviour model, Langevin equations, Personal mobility, Heterogeneous traffic conditions, Anticipation factors

1. Introduction

Recurrent and non-recurrent traffic congestion exacerbate air quality and road users' mobility in a metropolitan area around the world. In Australia, the Bureau of Infrastructure, Transport, and Regional Economics estimated A$16.3 billion of congestion cost in 2015 and predicted congestion costs to reach between A$27.7 and A$37.3 billion 2030 in BITRE (2015). Sydney's average travel speed not only declined by over 2km/h to 58.2km/h but also a percentage of free-flow speed has steadily declined by 0.6 per cent to 92.5 per cent from 2015 to 2018 in Bradley (2018). In recent years, the debut of information and communication technologies (ICT) in traffic engineering enables ones to relieve traffic congestion and resolve various byproducts of the congestion. Furthermore, the remarkable growths of ICT diffuse the international norm of transportation systems to pursue environmentally friendly, person-centred, and multi-modal systems to

*Corresponding author
Email addresses: seunghyeon.lee@uts.edu.au (Seunghyeon Lee), ryuri7@ajou.ac.kr (Ingon Ryu), dong.ngoduy@monash.edu (Dong Ngoduy), nam.hoang@monash.edu (Nam H. Hoang), keechoo@ajou.ac.kr (Keechoo Choi)

maximize safety, mobility, and efficiency in the systems. It introduces novel low-carbon transport modes, giving rise to new sensitive issues to a conventional urban road network. Consequently, it is inevitable to systematically analyse the behaviour of the newly introduced transport modals to tackle newly appeared conflicts among traffic modes and safety issues with understanding the stochastic behavioural characteristics of the new sustainable transport modes under mixed traffic conditions.

A low-carbon personal transport mode typically includes pedestrians, bicycles, and personal mobility (PM) devices, defined as E-scooters in this study. Transport for New South Wales (TfNSW) underlined the potential benefit of new personalised devices for short trips, such as E-bikes and E-scooters, in a metropolitan area in Constance & Pavey (2018), even if the use of E-scooters is prohibited in a public area in NSW as sharing economy. In the meantime, they mentioned it is required to create an appropriate environment where they could be ridden safely and efficiently to realise their potential benefits in the area of greater Sydney. Behavioural characteristics of pedestrians and bicycles have been thoroughly studied in recent decades. In contrast, there is plenty of room for investigating the behaviour of PM devices under mixed traffic conditions to promote its use in an urban road network to improve individual mobility and accessibility as a first-and-last mile trip among trip chains.

The debut of PM devices was debatable in many countries due to its vague definition and unexpected boom as sharing economy in an urban area, which could cause unpredictable conflicts to current transport modes and safety issues. Fletcher (2017) illustrates that a motorised scooter, which is not classified into road vehicles in Australia, means a device that is designed to be used by a single person, has two or more wheels and a footboard supported by the wheels, is steered by handlebars, and is propelled by a motor or motors having a combined maximum power output not exceeding 200 watts. Even if a wide range of PM devices are currently used in public spaces and vehicular road facilities to improve road users' mobility and accessibility in a complex urban network, the related laws and regulations are varied state-to-state in Australia. Its public use is strictly prohibited in NSW, South Australia, Western Australia, and ACT while it is conditionally or partially permitted in Queensland, Victoria, Northern Territory, and Tasmania. Thus, it is imperative to analyse and understand the stochastic behavioural dynamics of PM devices under mixed conditions of low-carbon transport modes to construct clear safety regulations and operational strategies in an urban road network.

Our study aims to develop a stochastic behavioural model of PM devices under heterogeneous traffic conditions in a shared lane based on car-following theories, which are at a mature level of studies to define dynamics of moving objects along with a designated lane in an area of traffic engineering. Treiber & Kesting (2018) and Kurtc & Treiber (2020) simulated bicycle traffic behaviour by the intelligent driver model (IDM) as well as examined the instabilities of the bike dynamics. They assumed that bicycles' dynamics, one of the leading sustainable transport modes, is not significantly different from vehicles' dynamics. Based on their validated assumptions and conclusions, we create a set of anticipation factors to tackle the sensitivity of PM devices' speed profiles against space headway and relative speed to the leading modes, including the same modes and the different modes in a shared lane. Such a set of variables will be then incorporated in the family of the optimal velocity model (OVM) and the full velocity difference model (FVDM). Moreover, experiments with the bicycles of Kurtc & Treiber (2020) and various PMs described in the ensuing paper exhibit stop-and-go waves of the PMs at a low-speed regime, similar to the instabilities of traffic flow in the recent experiments reported in Jiang et al. (2018). We thus extend a stochastic continuous differential equation developed in Ngoduy et al. (2019) and Lee et al. (2019) to capture such fluctuations in speed profiles of the PM devices in the heterogeneous low-carbon traffic flow.

To achieve the research goal, this article is organised as follows. The literature review for CF models and PM's behaviour models and experimental designs are described in Section 2 and 3, respectively, to find research gaps and contributions, which are illustrated in Section 4. The model formulation of stochastic heterogeneous-leaders behaviour of PMs is discussed in Section 5. The model performance in the real-world experiments and the calibrated and validated stochastic behaviour models of PM devices are illustrated in Section 6. Finally, Section 7 provides conclusions of this study and future research directions.

2. Literature review

To date, the dynamics of PM devices had not received as much attention as that of vehicles from both macroscopic and microscopic perspectives. Macroscopic models mainly deal with vehicular traffic-flow characteristics at a low level of detail, such as density, speed, and flow. In contrast, microscopic models illustrate the dynamics of traffic flow at a high level of detail, including the behaviour of individual vehicles. A thorough understanding of the microscopic dynamics has enabled ones to establish safety standards to promote the effective management and operational strategies of traffic systems. Over the past decades, car-following (CF) and lane-changing (LC) models have separately explained the longitudinal and lateral, respectively, the behaviour of individual vehicles, even if it has been rare to define the simultaneous two-dimensional vehicular behaviour. In this paper, the CF theory is chosen for developing behaviour models of PM devices under heterogeneous traffic conditions.

In addition to the CF theory, we employ the Langevin approach, which is the form of stochastic differential equations used in physics, chemistry, financial economics, to capture the existing uncertainty in riding manoeuvres, rider's perception in PM behaviour modelling, and the effect of lateral interactions. Moreover, it is not possible to model the behaviour of PM devices without considering mixed traffic conditions because PM devices have always mingled with the current transport modes such as bicycles and pedestrians on shared footpaths and bicycle lanes in the real world. Consequently, we comprehensively reviewed the stochastic CF models, heterogeneous traffic conditions, and current behaviour models of low-carbon transport modes in the following subsections to define research gaps and significant contributions to the proposed study.

2.1. Stochastic car-following models

A concept of CF theories has been widely used to illustrate longitudinal interactions of vehicular movements on the road. In contrast, lateral interactions of vehicular movements have been mainly defined by LC models (see Zheng (2014)). CF models have mainly dealt with microscopic vehicular longitudinal behaviour through defining the reaction of the following vehicle concerning its neighbouring vehicles, including the individual speed and acceleration profiles (see Treiber & Kesting (2013) and references therein). Pipes (1953) introduced an idealised law of separation that the following vehicle maintains a sufficient distance from the leading vehicle. Its debut has led a considerable number of mathematical frameworks to define CF behaviour under a wide range of traffic flow and geometry conditions. Chandler et al. (1958), Gazis et al. (1961), and Herman (1959) proposed a simple linear CF model, the Gazis-Herman-Rothery (GHR) model, and Helly (1959) introduced the speed of the following vehicle in the desired following distance into the GHR model. A safety distance model was introduced in Kometani (1959) to assume that the follower reacts to maintain a relative distance with the preceding vehicle, whereas Newell (1961) and Gipps et al. (1981) proposed a non-linear function of the safety distance model.

In addition to the traditional paradigm of CF models, Treiber et al. (2000) developed the IDM to consider the desired space headway and the free flow speed to promote realistic acceleration and deceleration of a vehicle. Treiber et al. (2006) illustrated the desired time gap as a dynamic function of a speed variance, which was introduced in the IDM to represent several significant traffic phenomena: widely scattered flows, capacity drops, and platoons as effects of variance-driven time gaps. Bando et al. (1995) introduced the optimal velocity model (OVM), in which a vehicle is supposed to have an optimal velocity decided by the space headway from the leading vehicle. For the following vehicle in the OVM, the difference between the optimal velocity and the actual velocity has a significant impact on its acceleration profile. Bando et al. (1998) improved the OVM to involve driver reaction time. Meanwhile, their parameters were calibrated in Helbing & Tilch (1998). Furthermore, Jiang et al. (2001) proposed a full velocity difference model (FVDM) to introduce relative speed's effect on the acceleration. Based on the LWR theory in Lighthill & Whitham (1955) and Richards (1956), Newell (2002) proposed the simplified CF model, in which the spatiotemporal trajectories of the following vehicle are identical to that of the preceding vehicle under steady-state traffic conditions. In addition to these existing elementary car-following models, there have been a vast number of other CF models, which were extended to cover a wide range of traffic problems such as multi-class vehicles, multi-anticipations, delayed responses, connected vehicles, etc. (Kesting & Treiber, 2008; Ngoduy, 2015b,a; Jia & Ngoduy, 2016b,a; Ngoduy, 2013; Treiber et al., 2005; Jia et al., 2019; Sun et al., 2018).

To analyse driving behaviour in non-lane based mixed traffic, Gunay (2007) introduced the lateral discomfort to CF models through a function of the off-centre effects of its leading vehicle. Moreover, Jin et al. (2010) proposed non-lane-based FVDM to confirm that the lateral separation effects greatly enhance the realism of car-following models. Ravishankar & Mathew (2011) modified the Gipps CF model to consider different vehicle types under heterogeneous traffic conditions. They showed that vehicle-type-varied parameters in the CF model are effective to enhance the prediction of the followers' behaviour in a shared lane. Moreover, Metkari et al. (2013) introduced lateral interactions between vehicles to the existing CF models to tackle characteristics of non-lane based heterogeneous motorised traffic flow. Li et al. (2015) proposed the novel CF model to consider the effects of two-sided lateral gaps in a shared lane based on a form of CF models. The proposed model described larger stable regions than the traditional form of CF models.

The dynamic desired time-headway and stochastic continuous driver's desired acceleration were introduced in the existing models to improve the performance of CF models. Jabari & Liu (2012, 2013) have considered the source of randomness in the first order continuum model (i.e. LWR model) by the uncertainty inherent in a driver gap choice, which is represented by random state-dependent vehicle time headway. In this model, the problem of negative sample paths of the stochastic variables is well tackled. Zheng et al. (2018) proposed a Lagrangian model to describe the uncertainty of the following vehicle's free-flow speed, reaction times, and safe distance to the leading vehicle. Zhou et al. (2017) compared the IDM and recurrent neural network (RNN) to predict traffic oscillations, meanwhile, Tian et al. (2016a,b) considered high-speed and low-speed driving behaviour, separately, to improve performance of the IDM. A stochastic desired acceleration was introduced in the simplified CF model in Laval et al. (2014), which illustrated quantitative relationships between CF theories and traffic oscillations due to the inherent stochasticity of human driving behaviour. Treiber & Kesting (2018) carried out the stochastic stability analysis of CF models to analyse trajectories of two consecutive vehicles in a specific CF theory derived from an acceleration-based model.

A distinct approach proposed in Ngoduy et al. (2019) applied Langevin equations to capture the stochastic driving behaviour in the OVM by using an extended Cox-Ingersoll-Ross (CIR) stochastic process. Based on the model of Ngoduy et al. (2019), Lee et al. (2019) integrated deep learning methods and the multi-lane stochastic CF model to describe traffic dynamics under a multi-lane traffic environment. Apart from the model of Ngoduy et al. (2019); Tian et al. (2019); Zheng et al. (2020), most existing stochastic car-following models show that the stochasticity does not contribute to the instability of traffic flow, which do not conform to the empirical findings by Jiang et al. (2018) where it does affect the traffic instabilities in the low-speed regime. To the best of our knowledge, the work in Ngoduy et al. (2019); Tian et al. (2019) is among very few attempts to show the noise-induced instability of traffic flow in the low-speed regime analytically using a microscopic model. In this study, we thus extend the method in Ngoduy et al. (2019) to developing a stochastic continuous CF framework to model the PM behaviour under mixed traffic conditions. The proposed framework aims to tackle the behavioural uncertainty of PM riders, pedestrians, and bikes within the shared footpath area.

2.2. Behaviour models of low-carbon personal transport modes

Diverse research approaches have been proposed to analyse behavioural characteristics of sustainable personal transport modes for the last several decades. For the majority of green transport modes, including pedestrians and bicycles, microscopic dynamics of pedestrians have been actively studied in Helbing & Molnar (1995), Antonini et al. (2006), Papadimitriou et al. (2009), Asano et al. (2010), Kneidl et al. (2013), Guo et al. (2016), Zeng et al. (2017), and Xiao et al. (2019), whereas Heinen et al. (2010), Twaddle et al. (2014), Hoogendoorn & Daamen (2016), Zhao & Zhang (2017), Treiber & Kesting (2018), Mohammed et al. (2019), and Paulsen et al. (2019) have defined bicycles' spatiotemporal dynamics. Moreover, Tordeux & Schadschneider (2016) applied OVM to analyse the pedestrian's behaviour.

In the meantime, there is plenty of room for modelling micro-behavioural dynamics of PM devices, which mainly define E-scooters and E-bikes, unlike that of pedestrians and bicycles until recently. Ulrich (2005) categorised personal electric vehicles (PEV) into stand-on-scooters, which is the almost identical term to PM devices in this study, sit-on scooters, and mobility scooters, according to technical specifications, involving maximum speed, cruising speed, size of wheels, gradeability, riding position, and terrain. Furthermore, the author illustrated several potential benefits of the PEV to users and society, including lower operating costs

than automobiles, use as auxiliary modes with transit and passenger cars, lower door-to-door travel times for short distance in a metropolitan area, reduction of air and noise pollution, and substitute mobility for the transport vulnerable. They found the social force model can be adapted to simulate Segway's behaviour toward pedestrians' behaviour. The effects of PM devices on traffic streams of pedestrians were evaluated by a personal space in Pham et al. (2015). The authors developed a simulation model of interactions between PM devices and pedestrians to show that PM devices significantly influence the increase in pedestrian density. Dias et al. (2018) explored the applicability of a social force model, which is used to model pedestrians' dynamics, for microscopic dynamics of Segway under mixed traffic conditions. Although they illustrated interactions between Segway riders and pedestrians using a social force model, they did not describe the inter-relationship of their behavioural dynamics under heterogeneous traffic scenarios. In addition, Hasegawa et al. (2018) analysed a danger perception of pedestrians toward PM devices under a shared footpath.

3. Circular experimental design

To calibrate and validate the proposed stochastic behavioural model of PM devices under heterogeneous traffic conditions, we designed the circular shared road in which the circumference is 120 metres, and the width is 1.5 metres. We conducted these experiments in a circular pilot study road in May 2019. Heterogeneous Low-carbon transport flow includes scooter riders as a PM device, bicycle riders, and pedestrians. In the narrow pathway, we designed that PM devices can overtake pedestrians and bikes, whereas no modes can overtake PM devices.

Fifteen university students in the class of traffic flow theories at Ajou University in South Korea, participated in a series of experiments. They can easily understand research purposes and significance of the proposed experimental methodology since they have studied the importance of circular experimental design for passenger cars, basic CF models, and traffic flow theories in the class. In addition, they learn how to ride bicycles and E-scooters safely under mixed traffic conditions. Pedestrians and bicycle riders are instructed to not only keep the consistent travelling speed at the edge of the circular shared road but also avoid sudden manoeuvres to change riding direction and speed. We instructed PM riders to find their gap acceptance against the circular traffic stream when asked to penetrate the mainstream. When PM riders want to take over pedestrians and bicycle riders in the shared lane, they should give a short prior verbal notice to walkers and bike riders and then, take their actions gently. When PM riders are asked to leave the stream, they are instructed to accelerate their PM slightly and then, leave the stream smoothly without interrupting the leading and the following riders.

We set four initial traffic conditions, including three pedestrians walking, three bicycles riding, three low-speed scooters driving below 10 km/h, and three high-speed scooters driving over 10 km/h, respectively. After 2 minutes of four initial traffic conditions, scooter riders enter and leave the main circular stream every 2 minutes, approximately. We allow a maximum of 10 modes running in the circular road at all four traffic conditions, in which the maximum density is 83.3 people/km. In contrast, its minimum value is 25.0 people/km. Consequently, we create 32 different heterogeneous traffic conditions to analyse the stochastic behaviour of the PM devices thoroughly. The following table summarises the time duration of all experiments.

Table 1: A time duration of circular experiments

Density (per/km)	25.0	33.3	41.7	50.0	58.3	66.7	75.0	83.3
3 bicycles + scooters	00:01:35	00:02:06	00:01:56	00:02:03	00:02:02	00:01:56	00:02:09	00:02:30
3 pedestrians + scooters	00:01:06	00:01:59	00:02:00	00:02:04	00:02:01	00:02:05	00:02:03	00:01:51
Low-speed scooters	00:02:21	00:01:45	00:01:58	00:01:58	00:02:04	00:02:05	00:01:53	00:02:04
High-speed scooters	00:02:33	00:01:50	00:01:58	00:02:09	00:01:55	00:02:03	00:02:00	00:01:55

Besides, we collect digital images recorded by a video camera installed at the top of a neighbouring building and a drone to extract the trajectories of all modes running along the track, which are illustrated in the following figure. A resolution of the extraction is 0.5 seconds. Meanwhile, the total number of frames

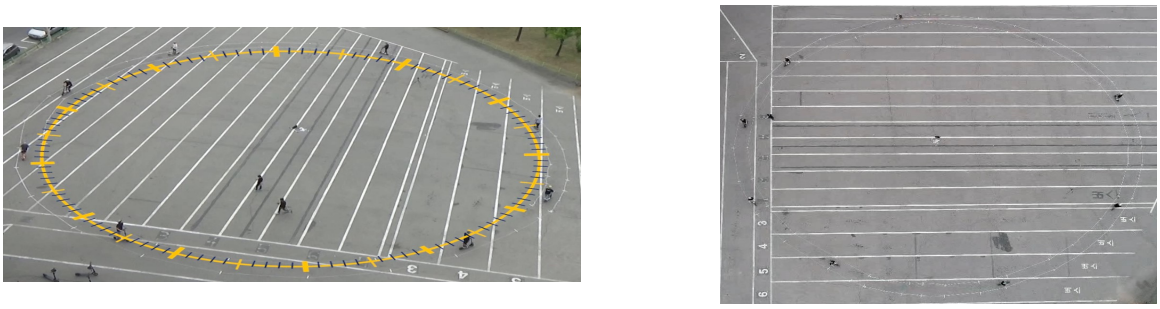

(a) A vision from the top of the building

(b) A vision from a drone

Figure 1: The samples of recorded digital images

per a single experiment is from 132 to 300 frames. Moreover, the extracted trajectories per 0.5 seconds of the individual PM device of 28 riders (7 riders x 4 experiments = total 28 riders) are used to construct stochastic behaviour models of sustainable modes under the circumstance, in which the leading PM device leave and enter the circular road.

In Fig. 1a, we create the graduation along the circle on the recorded video images to calculate the travel distance of the individual PM device per 0.5 seconds. We use the calculated travel distance in a 0.1 metre resolution to approximate the discrete values of the speed in 0.1m per 0.5s resolution. Besides, the recorded video images from the drone are used to calibrate the calculated travel distance based on the real travel distance to minimise the observed errors caused by the tilted angle of cameras in Fig. 1b.

4. Research gap

We discover several significant research gaps from the comprehensive review studies to propose a novel mathematical framework for modelling microscopic dynamics of PM devices through the designed experiment. To the best of our knowledge, stochastic behavioural characteristics of PM devices have never been captured from the perspective of PM riders against different low-carbon modes under narrow shared pathways. We carried out the real-world circular experiments to verify the effectiveness of the stochastic CF models in explanations of the behaviour of PM devices under heterogeneous flow conditions.

4.1. Oscillations of the PM speed at the low-speed regime in a single shared lane

Four initial traffic conditions, including three pedestrians walking, three bicycles riding, three low-speed scooters driving below 10 km/h, and three high-speed scooters driving over 10 km/h, respectively, are constructed to analyse oscillations of the PM speed at the low-speed regime in a single shared lane. The following figures provide oscillations of PM speed profiles under four hetero- and homogeneous traffic conditions.

We illustrate the oscillations of speed profiles of PM devices at the low-speed regime, which is similar to vehicular traffic behaviour where the stochastic behaviour plays a significant role in the instabilities at the low-speed regime.

In Fig. 2, Bike01, Bike02, and Bike03 at a Y-axis show speed profiles of bikes running below 5m/s the circle as the initial heterogeneous condition over 1,800 seconds. In the meantime, PM01 to PM07 show speed oscillations of PM devices at low-speed regime under bike-mixed traffic conditions. Primary traffic disturbances that scooter riders participate in and leave the traffic stream have a significant influence on speed oscillations of PM devices such as speed profiles of PM01 at 200s, PM05 at 1200s, and PM06 at 1400s.

In Fig. 3, low-speed profiles of pedestrians walking below 2m/s are illustrated in rows of Ped01, Ped02, and Ped03 marked at a Y-axis. They describe relatively constant speed profiles of pedestrians walking along with the circle as the initial heterogeneous condition, whereas they are highly disturbed after PM07 participated in the traffic stream at 1600s. Furthermore, graphs of PM01 to PM08 show speed oscillations of PM devices at low-speed regime under pedestrian-mixed traffic conditions. Speed profiles of PM devices

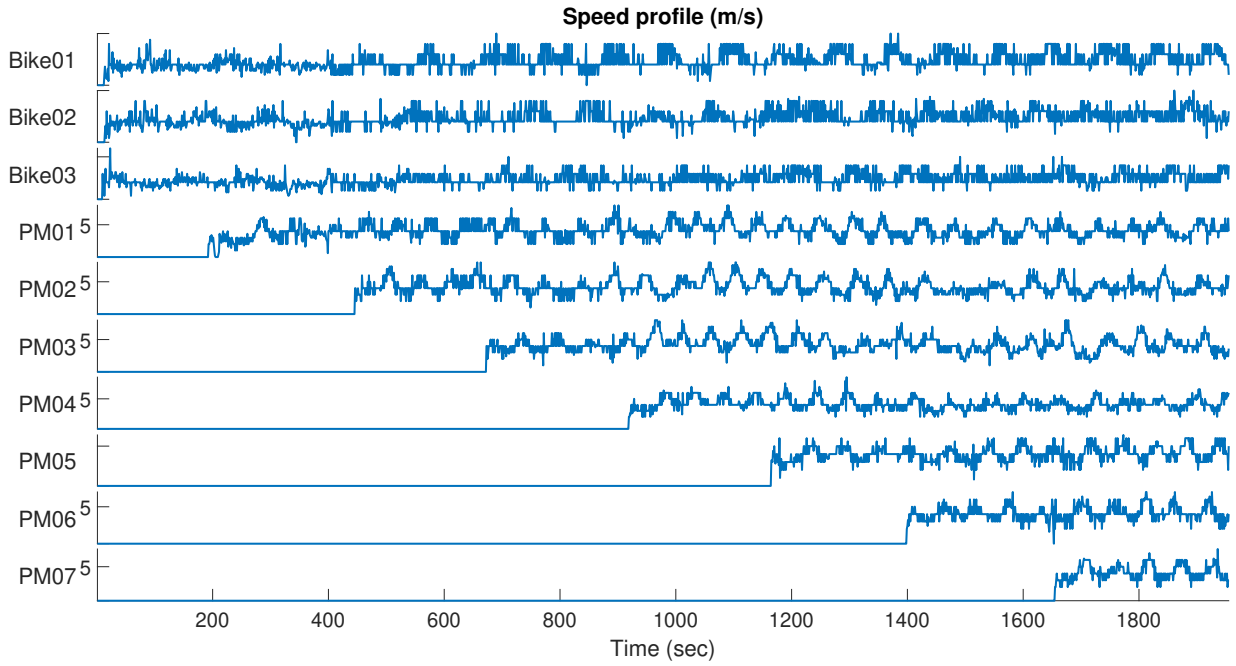

Figure 2: Speed oscillation of PM devices at low-speed regime under bike-mixed flow

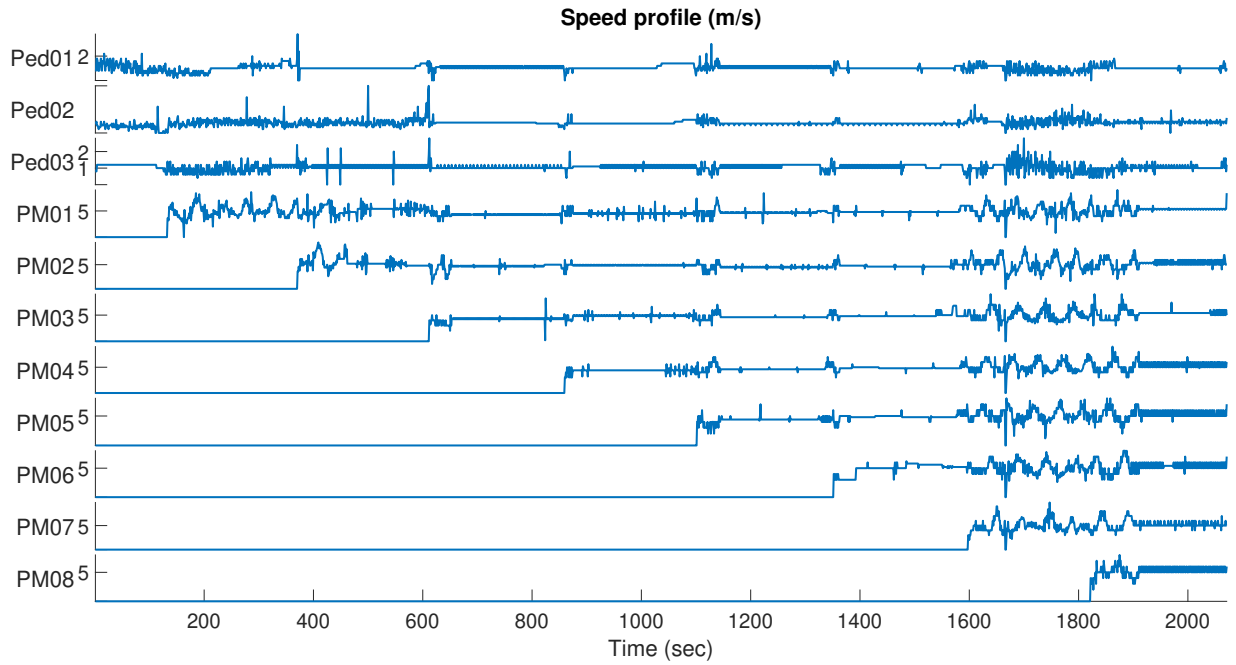

Figure 3: Speed oscillation of PM devices at low-speed regime under pedestrian-mixed flow

are extremely disturbed when PM01, PM07, and PM08 participated in the traffic stream at 200s, 1600s, and 1800s, respectively.

PM01, PM02, and PM03 denote speed oscillations of initial PM devices running below 5m/s and below 10m/s in Fig. 4 and Fig. 5, respectively.

In Fig. 4, PM02 and PM03 left the steam at 2300s and 2500s, respectively. Moreover, PM04 participated

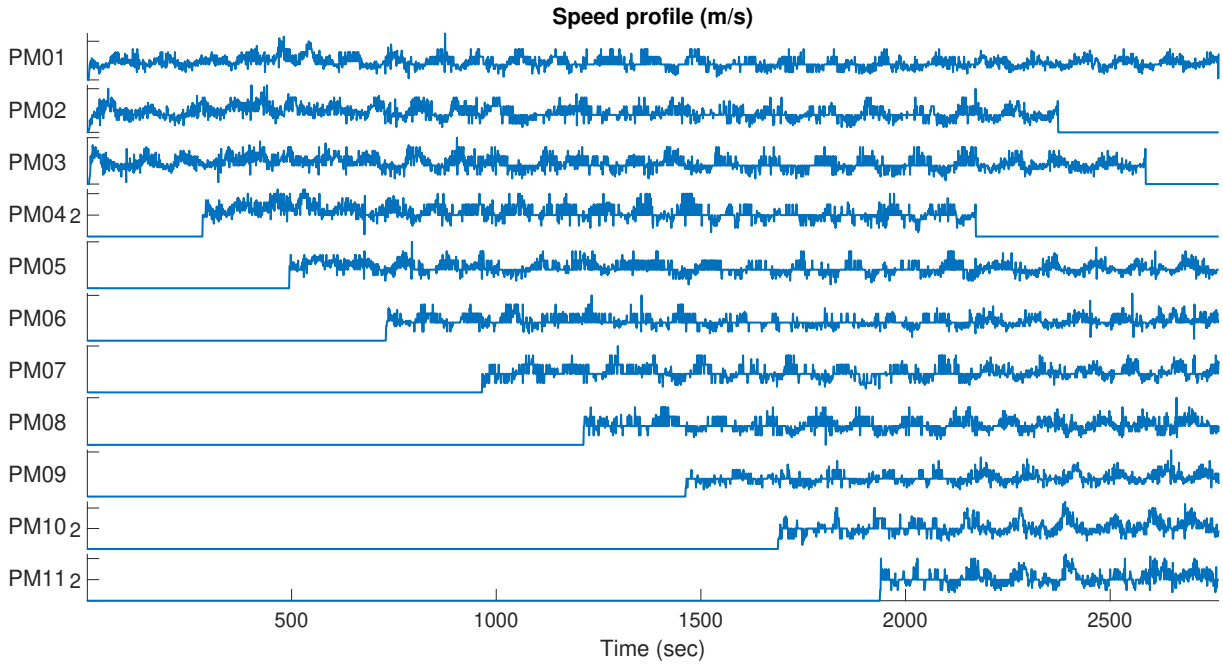

Figure 4: Speed oscillation of PM devices at low-speed regime under low-speed flow

in the mainstream at 300s and then, left from the stream at 2200s. Other PM devices participated in the stream around every 2 minutes, approximately, and the density of the low-speed running homogeneous PM stream varied from 25person/km to 83.3person/km. Their speed profiles are unstable at low-speed regime below 1m/s of speed when there is the new PM device in the stream or sudden changes in speed of the leading PM device such as speed profiles of PM03 at 300s, PM04 at 700s, PM05 at 700s, PM06 at 2400s, 2500s, and 2800s, PM08 at 1800s, and PM10 at 1700s.

Fig. 5 illustrates high-speed driving PM devices between 5m/s and 10m/s for the experimental period. PM06 and PM07 participated in the stream at 700s and 1000s and then left from the stream at 2400s and 2200s, respectively. Other PM devices gradually entered the mainstream and then, they were encouraged to maintain relatively high-speed driving below 10m/s. Although PM riders are allowed to increase their speed above 5m/s, their riding speed profiles are occasionally disturbed and decrease below 1m/s when the leading PM device suddenly changed their riding speed, and additional PM devices joined the traffic stream.

Consequently, the oscillations of the PM speed at the low-speed regime are similar to vehicular traffic where the stochastic behaviour plays a role in the instabilities at the low-speed regime, which are described in Jiang et al. (2018). Moreover, these oscillations are significantly influenced by mixed low-carbon modes flow and by additional PM devices joined in. Since the oscillations of PM devices are not reproducible with the deterministic form of CF models, the development of stochastic behaviour models of PM devices is significant to tackle uncertain changes in speed profiles of PM devices under diverse mixed traffic conditions. Moreover, the stochastic force is used to capture PMs' characteristics against movements of other PMs, pedestrians, and bicycles, and the effect of lateral interactions.

4.2. Purpose and contributions

The purposes of this study are thus to create a stochastic continuous heterogeneous PM devices-following model to cope with longitudinal interactions between different green transport modes in a shared lane. The proposed PM behavioural model tackles unpredictable fluctuations in the velocity of PM devices against relative speed and space headway to surrounding low-carbon modes under heterogeneous traffic conditions. In particular, there are four primary contributions of this study as follows:

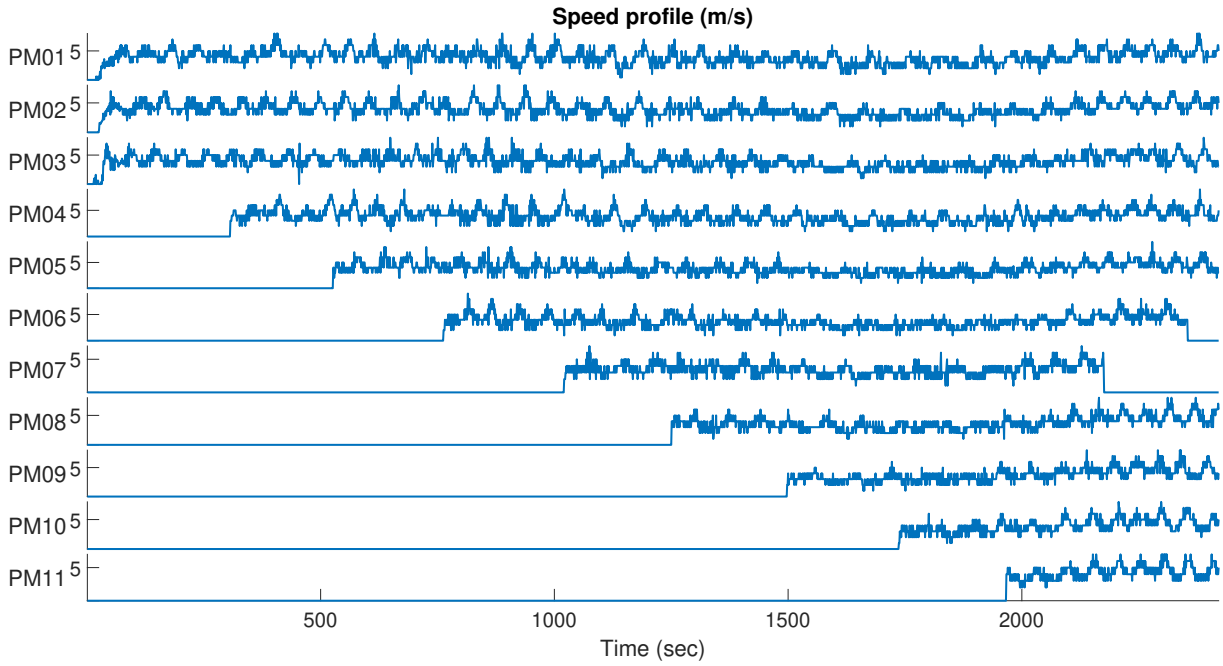

Figure 5: Speed oscillation of PM devices at low-speed regime under high-speed flow

- stochastic volatility derived from interactions between intra- and inter-sustainable modes is explained by the Langevin force in the proposed behavioural model of PM devices;
- Anticipation factors define a degree of influence of space headway and relative speed to the leading modes on the following PM device in the PM devices-following equation;
- The proposed stochastic models deal with not only fine fluctuations in PM speed profiles with the anticipation factors but also the main streams under diverse traffic density conditions;
- Real-world circular experiments are designed and carried out to calibrate and validate the proposed model;

To verify the effectiveness of the created stochastic behaviour models of PM devices, its performance compared to the existing models are given in the following sections.

5. Model formulation

This section presents the mathematical framework of a behaviour model of PM devices under mixed traffic conditions with stochastic volatility. The proposed framework creatively includes a concept of anticipation factors for space headway and relative speed against hetero- and homogeneous sustainable modes and stochasticity in the primary form of CF models. The definitions of the common indices, parameters, and variables used in this study are given in Table 2. Based on the common terms, a typical schematic configuration of the PM behavioural model is illustrated in Fig. 6. In Fig. 6, mode m, $m+1$, and $m+2$ are a PM device, a bicycle, and a pedestrian, respectively, within of a shared lane with w width. The nth PM device m is the target mode, which is moving at speed $v_{n,m}(t)$ and acceleration $a_{n,m}(t)$ at time t. Its intra-space headway to the leading PM is $s_{n,m}(t)$, whereas its inter-space headway to the leading bicycle and pedestrian is expressed as $s_{n,m+1}(t)$ are $s_{n,m+2}(t)$, respectively.

We suppose a sensitivity level could be varied toward space headway and relative speed among the same modes and between different modes in a shared lane. To facilitate this assumption, the integrated

Table 2: Index, Variables, and Parameters used for modelling

Index	
n	personal mobility devices
m	a group of low-carbon transport modes
t	time instant (s)
Variables and parameters	
$x_{n,m}(t)$	the position of device n in a group of mode m at time t (m)
$v_{n,m}(t)$	the speed of device n in a group of mode m at time t (m/s)
$a_{n,m}(t)$	the acceleration of device n in a group of mode m at time t (m^2/s)
$s_{n,m}(t)$	the space headway to leading device $n-1$ of device n in a group of mode m at time t (m)
$\Delta v_{n,m}(t)$	the relative speed to leading device $n-1$ of device n and in a group of mode m at time t (m/s)
δ_m	the anticipation factors to speed of the follower against device in a group of mode m
λ_m	the anticipation factors to position of the follower against device in a group of mode m
$\eta_m(t)$	the stochastic process of acceleration of a group of mode m at time t
σ_0	the positive dissipation parameters of acceleration
$f(.)$	the deterministic drift of acceleration profile
$g(.)$	the stochastic force of acceleration profile
$dW_{n,m}$	the increments of a standard Wiener process of device n in a group of mode m
$V_{op}(s_{n,m})$	the space headway-dependent optimal velocity of PM devices (m/s)
V_0	the desired speed of PM devices (m/s)
C	the shape of the equilibrium flow-density relations of PM devices under free traffic conditions
b	the length scale, defining the transition regime for the s-shape function from $V_{op}(s_{n,m}) = 0$ to $V_{op} \to V_0$
γ	the constant sensitivity coefficient of the optimal speed of PM devices in a deterministic drift $(1/s)$
κ	the constant sensitivity coefficient of the relative speed of PM devices in a deterministic drift $(1/s)$

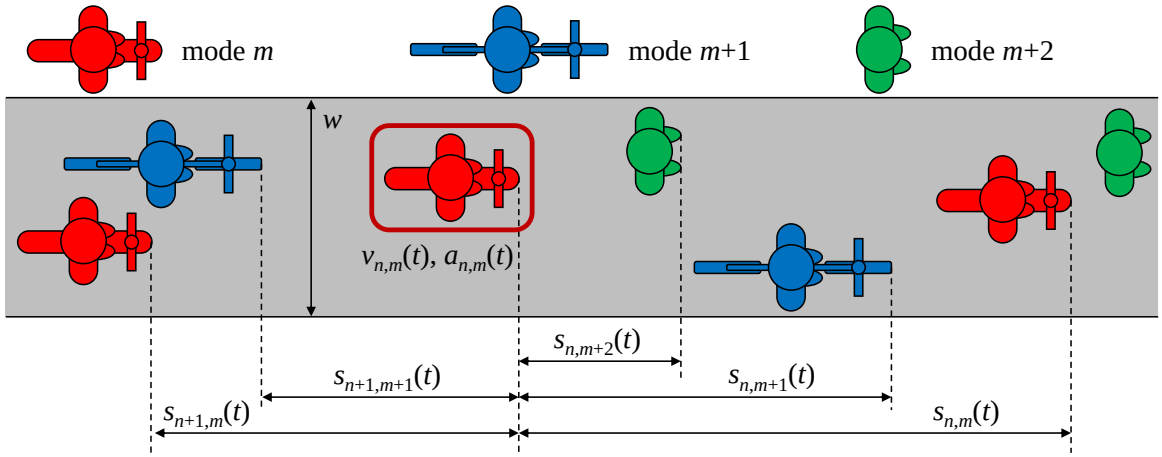

Figure 6: A typical configuration of the PM behaviour related to surrounding mixed low-carbon transport modes

mathematical framework is constructed to contain interactions of intra- and inter-modes simultaneously. We then formulate a form of stochastic differential equations (SDE) to capture the deterministic and stochastic characteristics of PM driving behaviour under mixed traffic conditions. Although Sugiyama et al. (2008) observed reaction time delays in dynamics of car-following behaviour on circular tracks, we suppose reaction time delay could have negligible impact in slow-moving systems below 20km/h, which is the low-carbon traffic flow in this study.

The multiplicative Gaussian white noise was used to illustrate the acceleration profiles of the following vehicles against the leading vehicles' speed profiles in the form of CF models justified in Laval et al. (2014). Based on a concept of the multiplicative Gaussian white noise, Ngoduy et al. (2019) and Lee et al. (2019) have adopted the Langevin equations to describe the stochastic behaviour of vehicles in the form of CF models to guarantee positive dissipation of speed profiles at a lower speed regime. The Langevin equations

have been widely used in physics, chemistry, mathematics, and financial engineering in the last decades, to describe the stochastic process, which is an effective method to model quasi-continuous diffusion processes. Furthermore, a random characteristic of the variance in the modelling of stochastic dynamics has captured the possibility of considering efficiently unpredictable and uncontrolled effects of exogenous variables, called stochastic volatility.

5.1. Car-following models

Let us recall a generic formulation of the (deterministic) car-following model for lane keeping vehicular driving behaviour as follows.

$$\frac{dv_n(t)}{dt} = f\left(v_n(t), s_n(t), \Delta v_n(t)\right) \tag{1}$$

where s_n and Δv_n represent, respectively, the space headway and the relative speed of vehicle n with its leading vehicle $n+1$ in the same lane. Note in this paper we define the relative speed as an approaching rate: $\Delta v_n = v_n - v_{n+1}$. The nonlinear function $f(.)$ depicts an elementary car-following model type such as the OVM, FVDM or IDM for vehicle n.

This elementary car-following model type is used to develop the stochastic behaviour model of the PMs in the ensuing section.

5.2. Stochastic behaviour model of PMs

To capture the non-lane disciplinary behaviour of the PMs as described in a shared lane as in Fig.6, we propose anticipation factors to define a level of recognition of the nth PM device in the mode m toward the leading PM devices, regardless of the mode type. To this end, the car-following model (1) is modified for PM device n in group m as below.

$$\frac{dv_{n,m}(t)}{dt} = f\left(v_{n,m}, \hat{s}_{n,m}, \Delta\hat{v}_{n,m}\right) \tag{2}$$

Similar to the car-following model, the function $f(.)$ describes the PM following behaviour of PM device n, which will be specified later.

Furthermore, the newly introduced variables $\hat{s}_{n,m}$ and $\Delta\hat{v}_{n,m}$ are the spatial average space headway and relative speed of PM n w.r.t. all the leading PMs, respectively, in the shared lane. Consider the the modes in Fig. 6, these variables are determined as follows:

$$\Delta\hat{v}_{n,m}(t) = \delta_m[v_{n,m}(t) - v_{n+1,m}(t)] + \sum_{m'\neq m} \delta_{m'}[v_{n,m}(t) - v_{n+1,m'}(t)] \tag{3}$$

$$\hat{s}_{n,m}(t) = \lambda_m[x_{n+1,m}(t) - x_{n,m}(t)] + \sum_{m'\neq m} \lambda_{m'}[x_{n+1,m'}(t) - x_{n,m}(t)] \tag{4}$$

where the physical meaning of the anticipation coefficient δ_m and λ_m $(m = 1, 2, 3)$ are given below.

In this study, we assume that the behaviour of the leading PM device and heterogeneous mode has a significant influence on the behaviour characteristics of the following PM device in a single shared lane. All low-carbon modes are running along in a shared lane, including undesignated lanes for a specific mode. In the shared lane, parallel running, overtaking the same modes or different modes, and following all modes are permitted in most countries. We introduce the anticipation factors, δ_m and λ_m, to the existing CF models to cope with these kinds of manoeuvres of sustainable modes. They are used to measure the sensitivity of the following PM device against space headway and relative speed to the leading same mode as well as different modes in a shared lane, separately. It is worth mentioning that Jin et al. (2010) introduced a single sensitive parameter in non-lane-based FVDM to enhance the performance of CF models for heterogeneous non-lane based vehicular traffic flow. The anticipation factors in our model are restricted to prevent over-quantifying the influence of relative speed and space headway toward the leading subjects on the following PM device. Furthermore, $v_{n+1,m}(t)$ and $v_{n+1,m+1}(t)$ describe the speed of the leading subjects involved in the same and the different group of modes, respectively, whereas $x_{n+1,m}(t)$ and $x_{n+1,m+1}(t)$ denote the location of the

leading subjects, respectively. The following constraints are imposed for these factors for 3 modes presented in Fig. 6:

$$\sum_{m=1}^{3} \delta_m = 1.0 \tag{5}$$

$$\sum_{m=1}^{3} \lambda_m = 1.0 \tag{6}$$

However, to simplify the numerical study in the next section, we only consider the interactions of the PMs (i.e. $m = 1$) and other mixed modes (i.e. $m = 2$).

To illustrate the stochastic PM behavioural model under heterogeneous traffic conditions, we extend the Langevin method proposed in Ngoduy et al. (2019) to describe the dynamics of PMs as follows.

$$dv_{n,m}(t) = f\left(v_{n,m}(t), \hat{s}_{n,m}(t), \Delta\hat{v}_{n,m}(t)\right) dt + g\left(v_{n,m}(t), \eta_m(t)\right) dt \tag{7}$$

where $g_{n,m}(.)$ is a stochastic force of the acceleration of PM n in group m, which depends on the traffic conditions with the stochastic process $\eta_m(t)$. This stochastic force is derived from the current speed of the subject mode.

In Eq. (7), the deterministic part could be governed by a specific definition of the function $f(.)$. Without loss of generality, we use the OVM and FVDM to represent the deterministic part in this study. To this end, the OVM and FVDM are modified, respectively, as follows:

- Extended OVM type:

$$f\left(v_{n,m}(t), \hat{s}_{n,m}(t), \Delta\hat{v}_{n,m}(t)\right) = \gamma\left[V_{op}(\hat{s}_{n,m}(t)) - v_{n,m}(t)\right] \tag{8}$$

- Extended FVDM type:

$$f\left(v_{n,m}(t), \hat{s}_{n,m}(t), \Delta\hat{v}_{n,m}(t)\right) = \gamma\left[V_{op}(\hat{s}_{n,m}(t)) - v_{n,m}(t)\right] - \kappa\Delta\hat{v}_{n,m}(t) \tag{9}$$

where optimal speed function V_{op} is defined as:

$$V_{op} = \frac{V_0}{2}\left[\tanh\left(\frac{\hat{s}_{n,m}}{b} - C\right) - \tanh\left(-C\right)\right] \tag{10}$$

.

In Eq. (7), we consider the stochastic force $g(.)$ to conform to multiplicative Gaussian white noises, which illustrates normally distributed fluctuations of behaviour:

$$g\left(v_{n,m}, \eta_m\right) = \sigma\left(v_{n,m}\right) dW_{n,m}(t) \tag{11}$$

where $W_{n,m}(t)$ shows the increment of a standard Wiener process (Uhlenbeck & Ornstein (1930)) to define the random deviations from the mean speed of the individual PM device n in the group m. $\sigma\left(v_{n,m}\right)$ denotes a positive speed-dependent dissipation parameter illustrating the noise intensity of PM n in group m, in which higher $\sigma\left(v_{n,m}\right)$ means more randomness in the acceleration of the following PM device.

To relax the assumption of the constant dissipation parameter and to enhance the positive constraints of the trajectories of the stochastic model variables, Ngoduy et al. (2019) proposed an extended Cox-Ingersoll-Ross (CIR) process (Cox et al. (1985)) to model the acceleration deviations in a stochastic OVM. In a similar line, in this study, we follow the extended CIR process to model the PM device behaviour under mixed traffic conditions as follows:

$$\sigma\left(v_{n,m}\right) = \sigma_0\sqrt{v_{n,m}} \tag{12}$$

where σ_0 is a noise strength coefficient. A primary advantage of adapting the modified CIR process in the SDE is to mitigate the negative trajectories of the stochastic variable $v_{n,m}(t)$ for any arbitrary values

of σ_0. This implies that σ becomes very small even for high values of σ_0 when $v_{n,m}(t)$ is close to zero. In this case, the stochastic model Eq. (7) is totally governed by the deterministic part. Furthermore, we set $V_{op} = max(0, V_{op})$ in the numerical implementation and the case study to prevent the negative speed due to numerical errors in the simulation. The proposed model is numerically simulated using a standard Euler–Maruyama scheme. We provided a detailed definition of the discretisation in the Appendix in the authors' previous study in Ngoduy et al. (2019).

6. Model performance in real-world experiments

We applied five different forms of models depending on stochasticity, relative speed, and anticipation factors, to the real-world circular experiments described in section 3. We divided the experimental data into calibration and validation sets to validate the effectiveness of the proposed methods.

Trajectories of PM devices are used to develop stochastic PM behaviour models and deterministic models based on the form of the OVM except for errors of digital image processing. Consequently, we compare the performance of the developed models illustrated in the following table to verify the excellent performance of the stochastic PM behaviour model compared to the deterministic PM models.

Table 3: Descriptions of the proposed models

	Model 1	Model 2	Model 3	Model 4	Model 5*
Stochasticity	✓	✓			✓
Relative speed			✓	✓	✓
anticipation factor	✓		✓		✓

In Table 3, we apply three different features: stochasticity, relative speed, and anticipation factors to the proposed models based on the OVM form. Stochasticity is considered in the models through the integrated form of PM behaviour models, involving the deterministic and the Langevin force. Relative speed is adopted as a form of FVDM, whereas anticipation factors measure influence on the following PM device from space headway and relative speed against the different leading sustainable modes in a shared lane. Individual trajectories of PM devices are used to establish individual stochastic models against each different traffic condition. Models 2 and 4 denote SOVM and FVDM, respectively, whereas anticipation factors are introduced in models 1 and 3 to examine the effectiveness of the newly developed sensitive coefficient considering speed profiles of the leading heterogeneous low-carbon modes. Consequently, models 5, considering stochasticity, relative speed, and anticipation factors induced by the heterogeneity of traffic flow, is the finally proposed stochastic PM behaviour models under mixed traffic conditions.

In the model calibration, the set of parameters in the proposed stochastic models are calibrated by a typical meta-heuristic optimization algorithm. We choose the Genetic algorithm (GA) for our illustration purposes, where 100 replications will be used in the stochastic simulation. We verified the excellent performance of model 5 by comparing it with other models in the model calibration process. After these comparisons, we used trajectories of PM devices 1, 3, 5, and 7 for global calibration processes of parameters in model 5, whereas PM devices 2, 4, and 6 for model validation.

The mean of the speed of individual sustainable modes (i.e. over 100 samples) is used to compare with the observed speed of individual modes where the (expected) total mean squared errors between the model output and the data is used as a performance index (PI) for mode $m = 1$, PM device:

$$PI = \sum_{n=1}^{N} \sqrt{\frac{1}{n} \sum_{t=1}^{T} \left[\hat{v}_{n,1}(t|\pi) - \tilde{v}_{n,1}(t)\right]^2} \tag{13}$$

where $t \in T$ is time step, $\hat{v}_{n,1}(t|\pi)$ denotes the mean simulated speed of the PM device n at time step t (over 100 samples) given the model parameter $\pi = [\delta_1\ \lambda_1\ \sigma_0\ V_0\ C\ b\ \gamma\ \kappa]$, depending on the sort of models

provided in Table 3. In contrast, $\tilde{v}_{n,1}(t)$ is the observed speed of the following PM device n at time step t. For we only consider the interactions of the PMs ($m = 1$) and other mixed modes ($m = 2$), the constraint of anticipation factors is reduced to: $\delta_2 = 1 - \delta_1$ and $\lambda_2 = 1 - \lambda_1$.

The proposed models in Table 3 are applied on trajectories of five PM devices at a time under four different traffic conditions in a case of individual calibration processes. Models 1, 2, and 5 illustrate the upper (95 percentile of confidence interval) and lower (5 percentile of confidence interval) bound, which depends on the estimated speed profiles of the following PM device.

6.1. PMs behaviour in bicycle-mixed conditions

We assume that bike-mixed traffic conditions have a significant impact on the stochastic behaviour of PM devices in addition to their deterministic behaviour. The stochastic force and anticipation factors are introduced in the form of the current CF models to capture the uncertainty of PM behaviour under bike-mixed traffic conditions.

6.1.1. Model calibration

We calibrate four models, which have different sets of parameters depending on the base model, in the following table. Table 4 provides mean values and standard deviations of parameters of seven PM devices for individual calibration processes to describe the heterogeneity of the parameters among PM riders under bike-mixed conditions.

In Table 4, mean values of the anticipation factors against space headway to the bike, δ_2, are 0.3284 and 0.0204 with 0.1509 and 0.0063 as standard deviations in Models 1 and 3, respectively. It is worth emphasising that space headway to the bike has a significant influence, around 30 percentile, on acceleration behaviour of PM devices under heterogeneous traffic circumstance in the form of stochastic differential equations, whereas not significant in model 3. Moreover, the values of positive dissipation parameters, σ_0, 0.15 - 0.19, show that behavioural uncertainty is well captured by the stochastic PM devices following models under mixed traffic conditions with lower standard deviations below 0.1. Mean values of the average desired speed of PM devices are between 5.0 and 5.3 m/s, which are identical to the specification of PM devices in a market. Moreover, standard deviations are varied from 0.55 to 1.1 in the average desired speed of PM devices. Values of a shape of the equilibrium flow-density relations, C, are stable in all models between 1.8 to 2.9 with 0.9 to 1.6 as standard deviations. The values of length scale, b, are between 2.5 and 4.7 with 0.5 to 1.5 as standard deviations. Meanwhile, the space headway coefficients, γ, are around 0.7 in models 1 and 2, whereas they are around 0.1 in models 3 and 4. The relative speed coefficient, κ, is 0.42 with around 0.2 as standard deviations in models 3 and 4.

Table 4: Calibration results under bicycle-mixed conditions

		Model 1	Model 2	Model 3	Model 4
δ_2	Mean	0.3284	n/a	0.0204	n/a
	SD	0.1509	n/a	0.0063	n/a
λ_2	Mean	n/a	n/a	0.0215	n/a
	SD	n/a	n/a	0.0106	n/a
σ_0	Mean	0.1507	0.1886	n/a	n/a
	SD	0.0858	0.0950	n/a	n/a
V_0	Mean	5.3006	5.1688	5.0038	5.1207
	SD	0.6411	0.8673	0.5597	1.0762
C	Mean	2.6737	2.8820	1.8316	2.7866
	SD	1.4185	1.3491	0.9318	1.5811
b	Mean	2.9523	4.7393	2.7813	2.5774
	SD	1.3653	1.1915	1.4630	0.5496
γ	Mean	0.7200	0.8991	0.1000	0.1000
	SD	0.6901	0.7296	0.0000	0.0000
κ	Mean	n/a	n/a	0.4215	0.4205
	SD	n/a	n/a	0.2074	0.2087

The fitted-trajectories of speed profiles of the third PM device are selected to compare the performance of the top three models in Table 4 in the following figure.

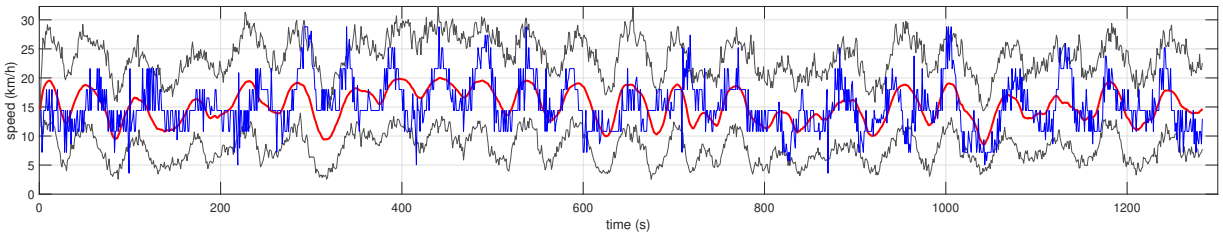

(a) Model 1 with stochasticity and anticipation factors

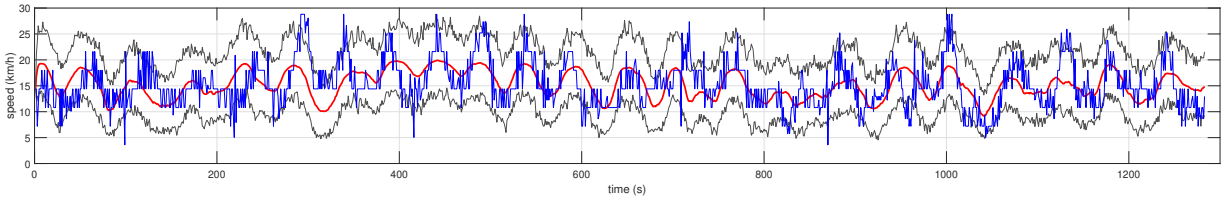

(b) Model 2 with stochasticity

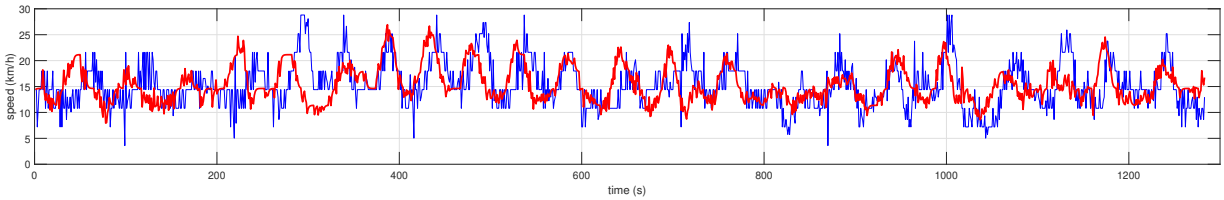

(c) Model 3 with relative speed and anticipation factors

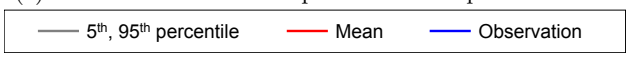

Figure 7: Speed profiles of the top three models in the third PM device under bike-mixed traffic conditions

Models 1, 2, and 3 are selected to describe the speed of the following PM device under bike mixed traffic conditions. In Fig. 7a, the proposed model 1 tackles all fine fluctuations in the speed of the following PM device through considering relative space headway to the leading PM and bike using anticipation factors, even if 5 and 95 percentile of variance is slightly wider than that of the model 2 due to considering relative space headway. In Fig. 7b, model 2 explains the main streams of speed with sufficient variance without anticipation factors; meanwhile, extensive fluctuations are not covered by model 2. According to the results of model 1 and 2, anticipation factors play a crucial role in behaviour models of PM devices under bike-mixed traffic conditions. In Fig. 7c, model 3 based on a concept of the FVDM enables to illustrate specific tendency in PM speed in the most periods with the anticipation factors, which measure a degree of sensitivity to space headway and relative speed against the leading PM and bike.

After comparing the performance of the top three models, we calibrate model 5, which is the finally proposed model, to consider stochasticity, relative speed, and anticipation factors with speed profiles of the second PM device in Table 5. For the second PM device, the traffic conditions are varied from the low-density mixed traffic condition, 33.3 $device/km$, to the high-density mixed traffic condition, 83.3 $device/km$ with three bikes running.

Table 5: Calibration results of the proposed model 5 under bike-mixed traffic conditions

	δ_2	λ_2	σ_0	V_0	C	b	γ	κ
Model 5	0.4161	0.0009	0.1276	5.5001	1.6079	9.2279	0.4496	1.4819

In Table 5, the anticipation factors for space headway, δ_2, and relative speed, λ_2, are 0.4161 and 0.0009, respectively. It is worth emphasising that space headway to the bike has a significant influence, around 40 percentile, on acceleration behaviour of PM devices under heterogeneous traffic circumstance in the form of stochastic differential equations, with anticipation factors for relative speed. Moreover, the value of positive dissipation parameters, σ_0, 0.1276, shows that behavioural uncertainty is well captured by the stochastic PM devices following models under mixed traffic conditions. The average desired speed of PM devices is 5.5 m/s, which are identical to the specification of PM devices in a market. Other calibrated variables of the finally proposed model 5 are slightly different from the previous models because it involves all anticipation factors and follows a form of stochastic differential equations. The statistics of calibration results are illustrated in the following table.

Table 6: Values of final value of GA of the models under bike-mixed traffic conditions

	Model 1	Model 2	Model 3	Model 4	Model 5
Final value of GA	8.8962	8.8966	5.2011	5.2011	4.107
Improvement than the base model	n/a	0.00%	41.54%	41.54%	53.83%

In Table 6, stochastic model 5 shows better performance than other models. Its final value of GA, 4.107, is greatly lower than others. This model type improves 53.83% compared to base model 1. Moreover, a form of FVDM, models 3 and 4, shows better performance than a form of OVM, models 1 and 2. Stochastic behavioural models of PM devices against heterogeneous traffic conditions perform better when combined with anticipation factors for both space headway and relative speed. The calibrated results are described in the following figures.

Fig. 8 illustrates that the stochastic FVDM (SFVDM) based behaviour model of PM devices captures the general tendency in speed profiles, whereas the upper and lower limits of speed could not cover all sudden fluctuations in several parts. This implies that newly created anticipation factors against space headway and relative speed to heterogeneous modes play a significant role in SFVDM to tackle partial influence on the behaviour of the following PM devices from the leading two different sustainable modes.

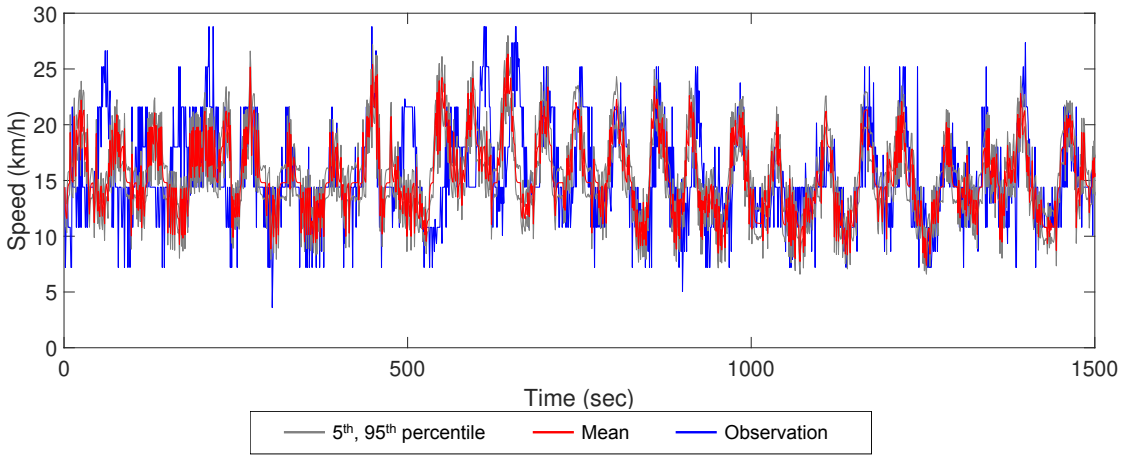

Figure 8: Performance of stochastic FVDM-based behaviour models of PM devices under bike-mixed traffic conditions

6.1.2. Model validation

Trajectories of PM devices 1, 3, 5, and 7 are used to globally calibrate model 5, including the stochastic force and two anticipation factors in the form of SFVDM. Those devices 2, 4, and 6 are used for model vali-

dation under bike-mixed heterogeneous conditions. The global calibration results of model 5 are illustrated in Table 7.

Table 7: Global calibration results of model 5 under bike-mixed conditions

	δ_2	λ_2	σ_0	V_0	C	b	γ	κ
Model 5	0.379	0.0000	0.2	4.5675	9.3087	1.4333	0.2292	0.9196

The globally calibrated parameters in Table 7 are slightly different from the parameters calibrated by trajectories of PM 2 only in Table 5 due to its diversity in the calibration set. The calibrated mean values of speed of PM 1, 3, 5, and 7 are provided with the upper (95 percentile of confidence interval) and lower (5 percentile of confidence interval) bound in Fig. 9. They are compared with the ground truth speed profiles of each corresponding PM device.

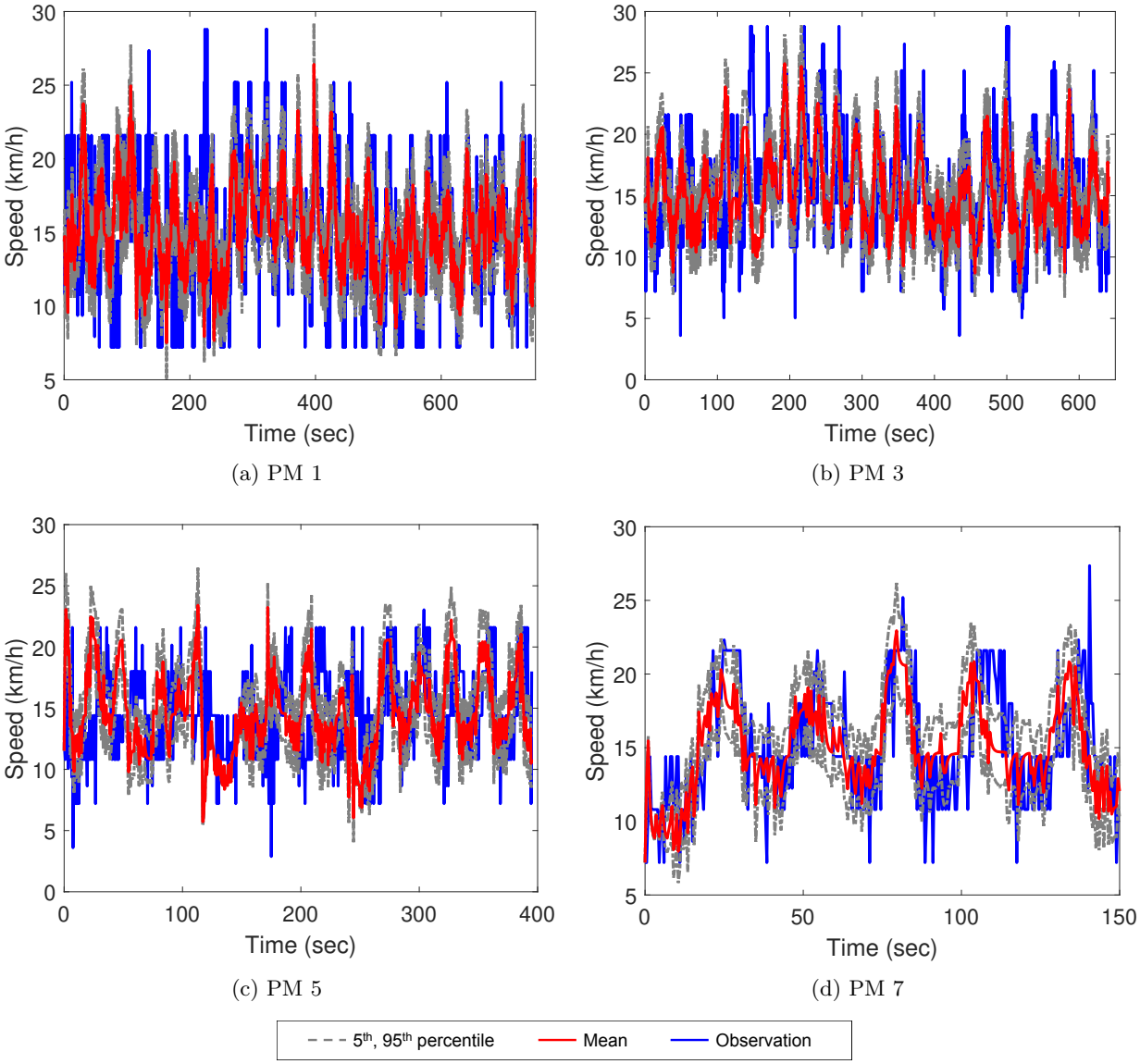

(a) PM 1

(b) PM 3

(c) PM 5

(d) PM 7

Figure 9: Global calibration results in bike-mixed conditions

In Fig. 9, the ground truth speed profiles of PM devices are within the upper and the lower stochastic bound of the estimated mean speed. Model 5 in global calibration can capture main fluctuations in speed profiles, whereas, it could not explain extreme manoeuvres across the PM devices. We validate the calibrated SFVDM with the ground truth speed profiles of PM devices 2, 4, and 6 in Fig. 10.

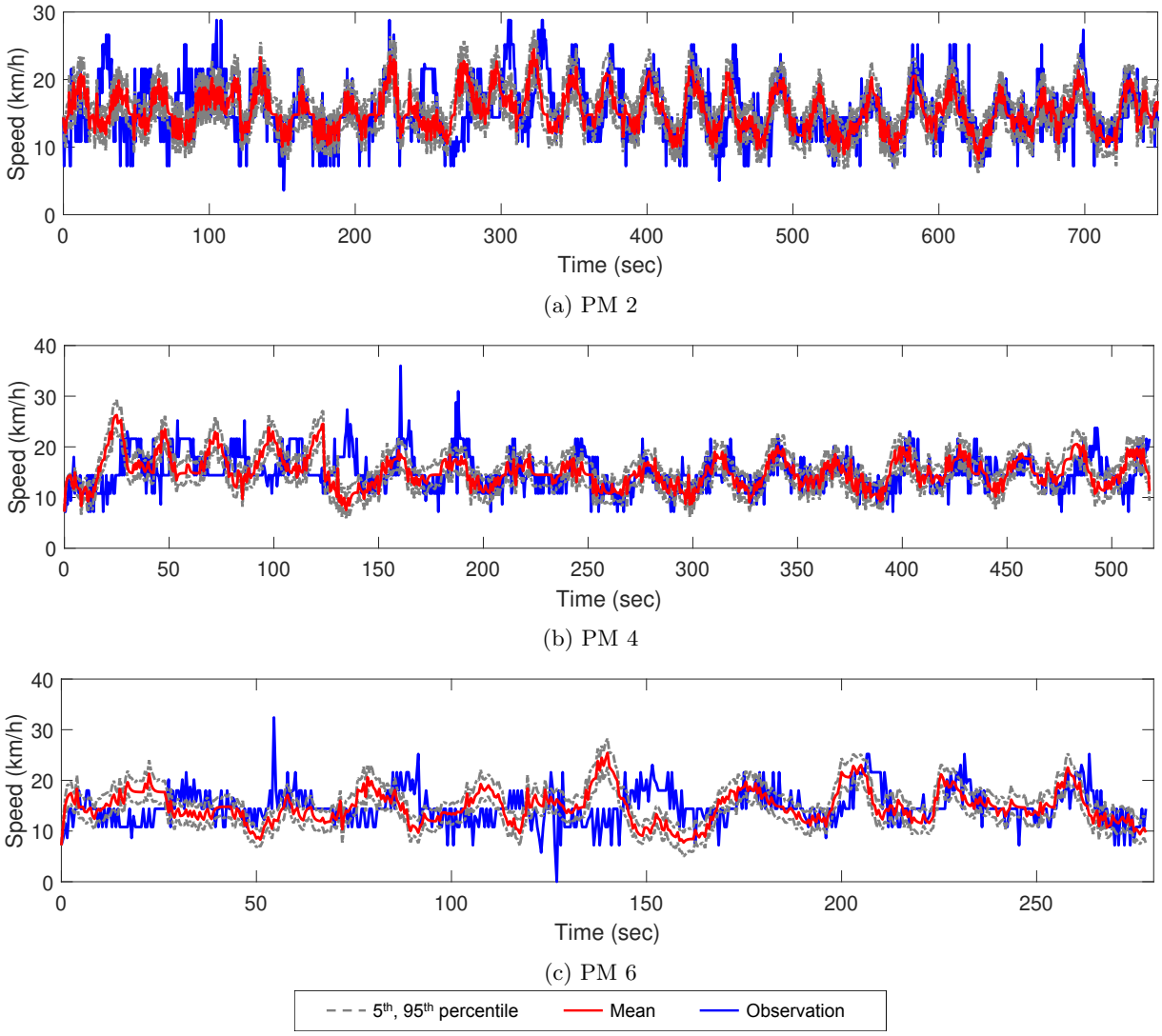

(a) PM 2

(b) PM 4

(c) PM 6

Figure 10: Model validation results of bike-mixed conditions

In Fig. 10, the proposed SFVDM captures the main streams of the observed speed of PM 2 and 4 within the upper and the lower bound of the mean speed. In contrast, the observed speed profiles of PM 6 are frequently beyond the upper and the lower bound of the estimated mean speed due to its relatively small sample size. Moreover, initial fluctuations in speed profiles are not illustrated well by model 5 in the validation set. In addition to the comparisons of speed profiles, we illustrate aggregated space headway to validate the excellent performance of the proposed model 5 in Fig. 11. The mean values of all moving trajectories estimated by model 5 are illustrated with observed moving trajectories of all PM riders under the bike-mixed scenario. Red and blue solid lines denote the moving trajectories estimated by model 5 and the observed moving trajectories, respectively.

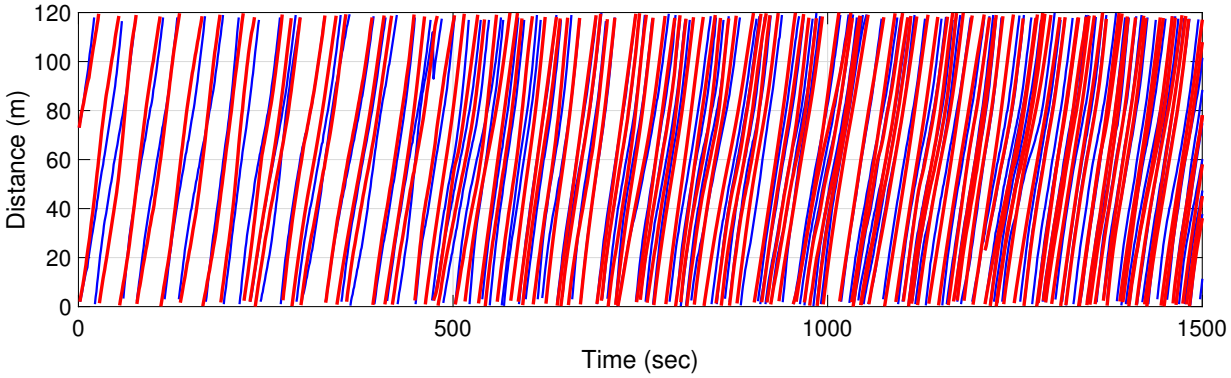

(a) Trajectories during a whole analysis period

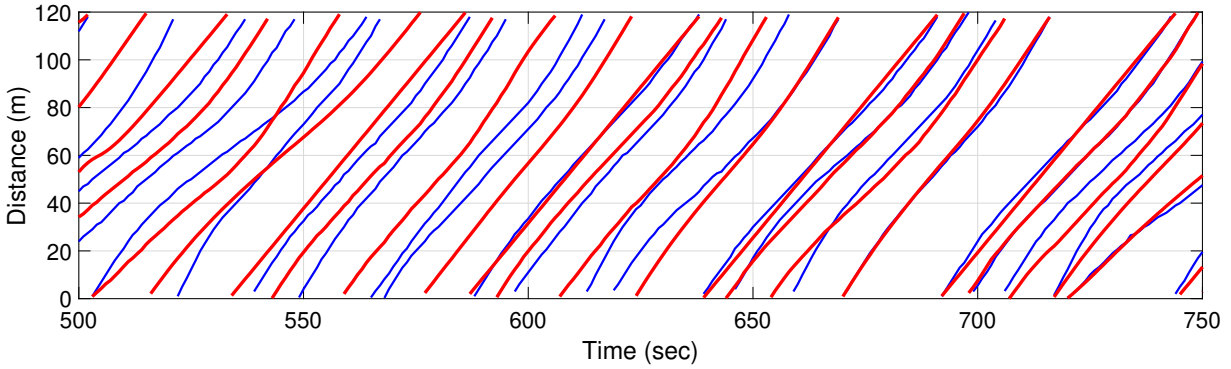

(b) Trajectories from 500s to 750s

Figure 11: the observed and the estimated moving trajectories under bike-mixed flows

In Fig. 11a, estimated main streams of spacing behaviour of PM devices are almost similar to the observed stream of spacing profiles under bike-mixed flow conditions. Moreover, the proposed SFVDM captures the spacing behaviour of PM riders newly joined or left, the leading riders, and the following riders at around 700s, 1000s, and 1500s. In Fig. 11b, the proposed model illustrates the spacing behaviour of PM devices, which is similar to the observed spacing trajectories from 500s to 750s, which is one of the highest density periods, whereas, the tiny fluctuations in the spacing profiles are not fully covered by the proposed model under pedestrian-mixed conditions.

6.2. PMs behaviour in pedestrian-mixed conditions

Stochastic behavioural models of PM devices show better performance than their original deterministic models under pedestrian-mixed traffic conditions. The stochastic force and anticipation factors are introduced in the form of the current CF models to capture the uncertainty of PM behaviour under pedestrian-mixed traffic conditions.

6.2.1. Model calibration

We calibrate five models, which have different sets of parameters depending on the base model, in the following table. The parameters are mean values in the case of individual calibration processes. Table 8 provides statistics of model parameters of seven PM devices for individual calibration processes to describe the heterogeneity of the parameters among PM riders under pedestrian-mixed conditions.

Table 8: Calibration results under pedestrian-mixed conditions

		Model 1	Model 2	Model 3	Model 4
δ_2	Mean	0.2403	n/a	0.0225	n/a
	SD	0.1362	n/a	0.0053	n/a
λ_2	Mean	n/a	n/a	0.0142	n/a
	SD	n/a	n/a	0.0030	n/a
σ_0	Mean	0.2448	0.2144	n/a	n/a
	SD	0.1841	0.1821	n/a	n/a
V_0	Mean	6.2567	6.2117	5.4130	5.5026
	SD	0.6141	0.6165	0.3924	0.8859
C	Mean	6.0506	6.0390	1.8059	1.6648
	SD	3.6362	2.5946	0.9110	0.6996
b	Mean	2.0980	3.2800	2.6284	2.6450
	SD	0.9454	2.0280	1.6709	0.9007
γ	Mean	1.7245	1.6440	0.3161	0.3162
	SD	0.5755	0.5647	0.0950	0.0952
κ	Mean	n/a	n/a	0.8340	0.8062
	SD	n/a	n/a	0.3181	0.3322

In Table 8, the anticipation factors against space headway to the leading pedestrian, δ_2, are 0.2403 and 0.0225 in Models 1 and 3, with small values of standard deviations, respectively. Although the space headway to the leading pedestrian has less influence on the speed of the following PM device than that to the leading bike in Section 6.1, it has a significant influence, around 25 percentile, on acceleration behaviour of PM devices under pedestrian-mixed traffic circumstance in the stochastic behaviour models, whereas not significant in model 3. Moreover, the values of the dissipation coefficient, σ_0, 0.21 - 0.24, in individually calibrated models with 0.18 of standard deviations, show that behavioural uncertainty is well captured by the stochastic PM devices following models under pedestrian-mixed conditions, even if they are larger than the case of bike-mixed conditions in Section 6.1. The average desired speed of PM devices is between 5.4 and 6.3 m/s with small values of standard deviations from 0.4 to 0.8, which are larger than the case of bike-mixed conditions within the designed specification of PM devices in a market, which is significantly different from the average desired speed of vehicles, 33 m/s. Values of a shape of the equilibrium flow-density relations, C, are significantly different between models, even if they are stable in all calibration cases with lower values of standard deviations. The values of length scale, b, are between 2.0 and 3.2, meanwhile, the space headway coefficients, γ, are between 0.3 to 2.0. Their values of standard deviations are varied from 0.9 to 2.0 and from 0.09 to 0.5, respectively. The relative speed coefficients, κ, are around 0.8 with 0.3 of standard deviations in Models 3 and 4. The fitted-trajectories of speed profiles are selected to compare the performance of the top three models in the case of the fifth PM device in Table 8 in the following figure.

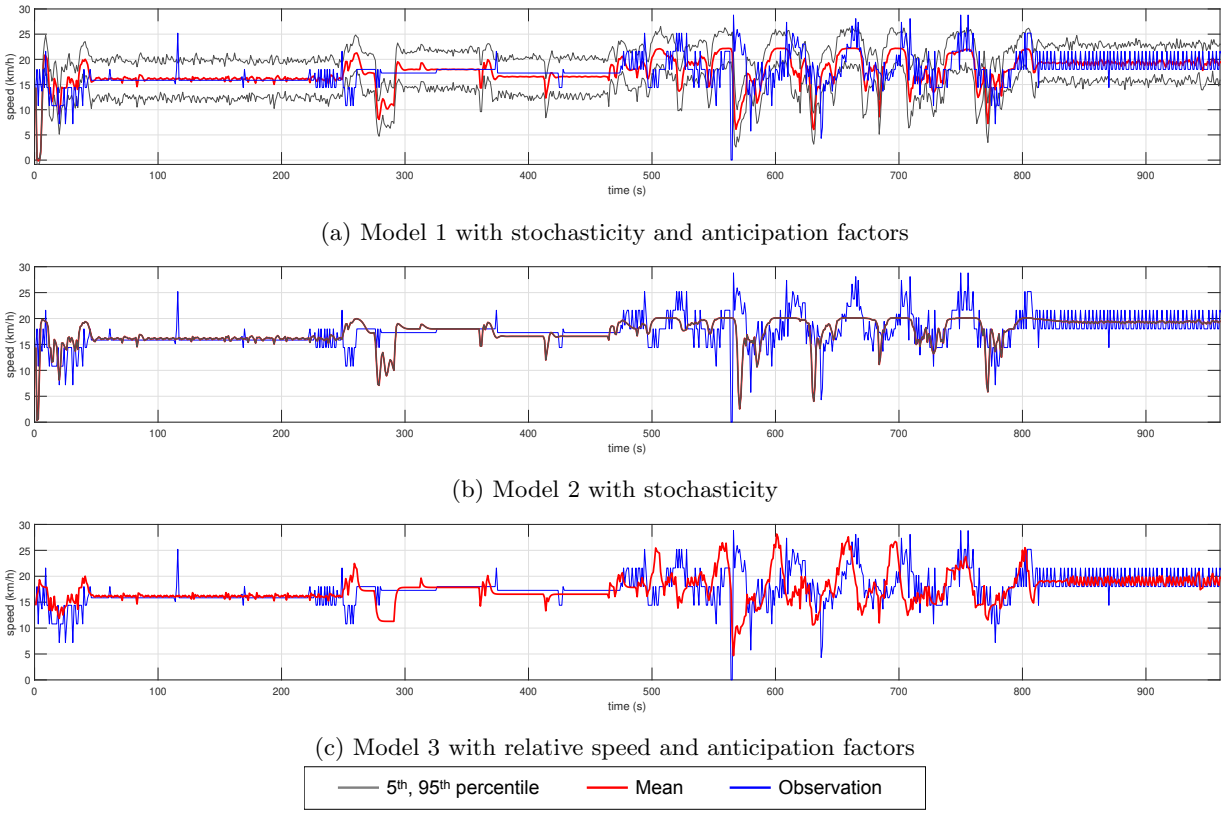

(a) Model 1 with stochasticity and anticipation factors

(b) Model 2 with stochasticity

(c) Model 3 with relative speed and anticipation factors

Figure 12: Speed profiles of the top three models in the fifth PM device under pedestrian-mixed traffic conditions

Models 1, 2, and 3 are selected as the top three significant models to describe the speed of the fifth PM device under pedestrian-mixed traffic conditions. In Fig. 12a, the proposed model 1 explains the main fluctuations in the speed of the following PM device through considering space headway to the leading PM and pedestrian using anticipation factors, even if the calibrated speed profiles miss some fine fluctuations in the real speed profiles. In Fig. 12b, model 2 captures only the mainstream of the speed profiles without considering anticipation factors. In Fig. 12c, model 3 tackles fine fluctuations in PM speed profiles in the most periods with the anticipation factors.

After comparing the performance of the top three models, we calibrate model 5 to not only consider the relative speed and space headway but also take into account a fine stochastic fluctuation of speed profiles under pedestrian-mixed conditions in the following tables and figures. For the second PM device, the traffic conditions are varied from the low-density mixed traffic condition, 33.3 $device/km$, to the high-density mixed traffic condition, 83.3 $device/km$ with three pedestrian walking.

Table 9: Calibration results of the proposed model 5 under pedestrian-mixed traffic conditions

	δ_2	λ_2	σ_0	V_0	C	b	γ	κ
Model 5	0.3176	0.0	0.5	6.7837	1.338	9.2094	0.4496	1.4819

In Table 9, the anticipation factors for space headway, δ_2, and relative speed, λ_2, are 0.3176 and 0.0, respectively. It is worth emphasising that space headway to the bike has a significant influence, around 30 percentile, on acceleration behaviour of PM devices under heterogeneous traffic circumstance, whereas relative speed against the leading pedestrian has no influence on the acceleration behaviour of the follower in the form of stochastic differential equations. Moreover, the value of positive dissipation parameters, σ_0,

0.5, shows that behavioural uncertainty is well captured by the stochastic PM devices following models under mixed traffic conditions. The average desired speed of PM devices is 6.8 m/s, which is within the specification of PM devices in a market. Other calibrated variables of the finally proposed model 5 are slightly different from the previous incomplete models because it involves all anticipation factors and follows a form of stochastic differential equations. The statistics of calibration results are illustrated in the following table.

Table 10: Values of final value of GA of the models under pedestrian-mixed traffic conditions

	Model 1	Model 2	Model 3	Model 4	Model 5
Final value of GA	6.7876	6.7803	6.3285	6.3285	6.0386
Improvement than the base model	n/a	0.11%	6.76%	6.76%	11.03%

In Table 10, stochastic model 5 shows better performance than other models. Its value of least square error, 6.0386, is lower than others between 6.3 and 6.8. Moreover, a form of FVDM, models 3 and 4, shows slightly better performance than a form of OVM, models 1 and 2. Stochastic behavioural models of PM devices against heterogeneous traffic conditions perform better when combined with anticipation factors for both space headway and relative speed. Under pedestrian-mixed traffic conditions, the effectiveness of stochasticity and anticipation factors is not as significant as them under bike-mixed conditions to improve model performance. In the experiments, we observed that PM riders tend to make their platoon to follow the leading PM device directly to minimise their distractions and anticipations caused by pedestrian movements and avoid direct conflicts with low-speed walking pedestrians alone. The calibrated results are described in the following figures.

In Fig. 13, the SFVDM based behaviour model of PM devices illustrates not only the main streams of speed but also tiny fluctuations in speed within the lower and upper bound of PM speed. This implies that newly created anticipation factors against space headway and relative speed to heterogeneous modes play a significant role in SFVDM to tackle partial influence on the behaviour of the following PM devices from the leading two different sustainable modes.

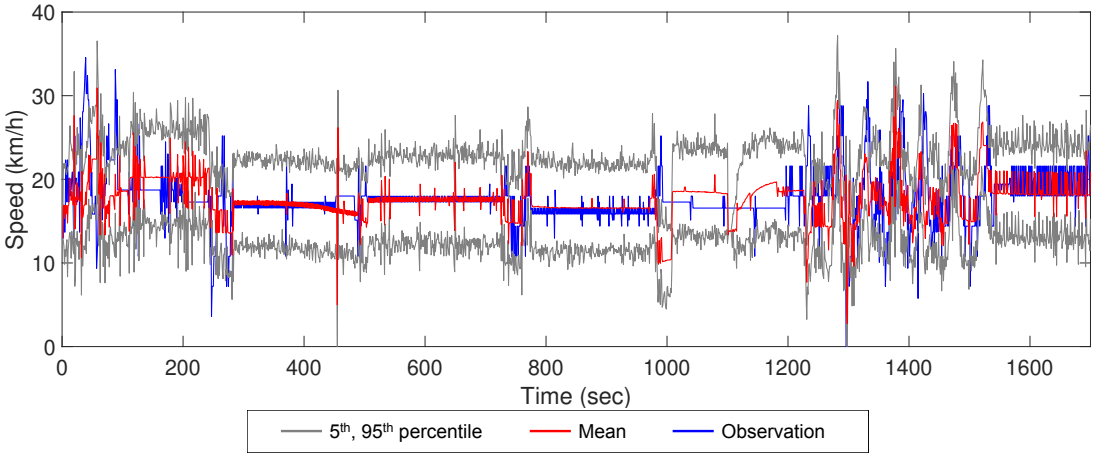

Figure 13: Performance of stochastic FVDM-based behaviour models of the second PM devices under pedestrian-mixed traffic conditions

6.2.2. Model validation

Trajectories of PM devices 1, 3, 5, and 7 are used to globally calibrate model 5, including the stochastic force and two anticipation factors in the form of SFVDM. Those devices 2, 4, and 6 are used for model

validation under pedestrian-mixed heterogeneous conditions. The global calibration results of model 5 are illustrated in Table 11.

Table 11: Global calibration results of model 5 under pedestrian-mixed conditions

	δ_2	λ_2	σ_0	V_0	C	b	γ	κ
Model 5	0.4659	0.0003	0.202	6.8173	2.751	5.7757	1.8264	0.2247

The globally calibrated parameters in Table 11 are slightly different from the parameters calibrated by trajectories of PM 2 only in Table 9 due to its diversity across PM devices under mixed conditions. The calibrated mean values of speed of PM 1, 3, 5, and 7 are provided with the upper (95 percentile of confidence interval) and lower (5 percentile of confidence interval) bound in Fig. 14. They are compared with the ground truth speed profiles of each corresponding PM device.

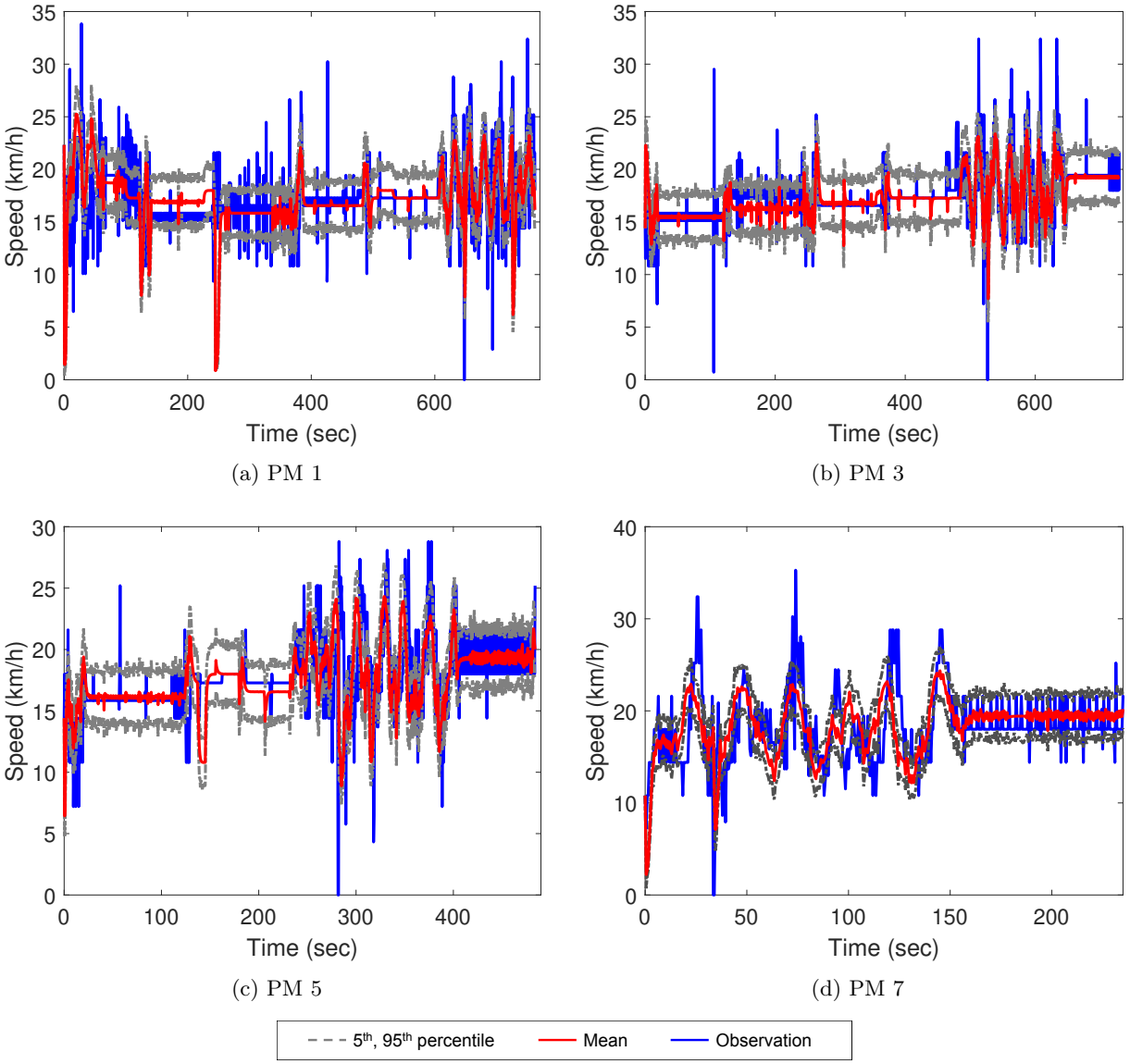

(a) PM 1

(b) PM 3

(c) PM 5

(d) PM 7

Figure 14: Global calibration results in pedestrian-mixed conditions

In Fig. 14, the most parts of the ground truth speed profiles of PM devices are within the upper and the lower stochastic bound of the estimated mean speed. Model 5 in global calibration well illustrates the primary fluctuations in speed profiles but it could not capture sudden changes in accelerations and deceleration. We validate the calibrated SFVDM with the ground truth speed profiles of PM devices 2, 4, and 6 in Fig. 15.

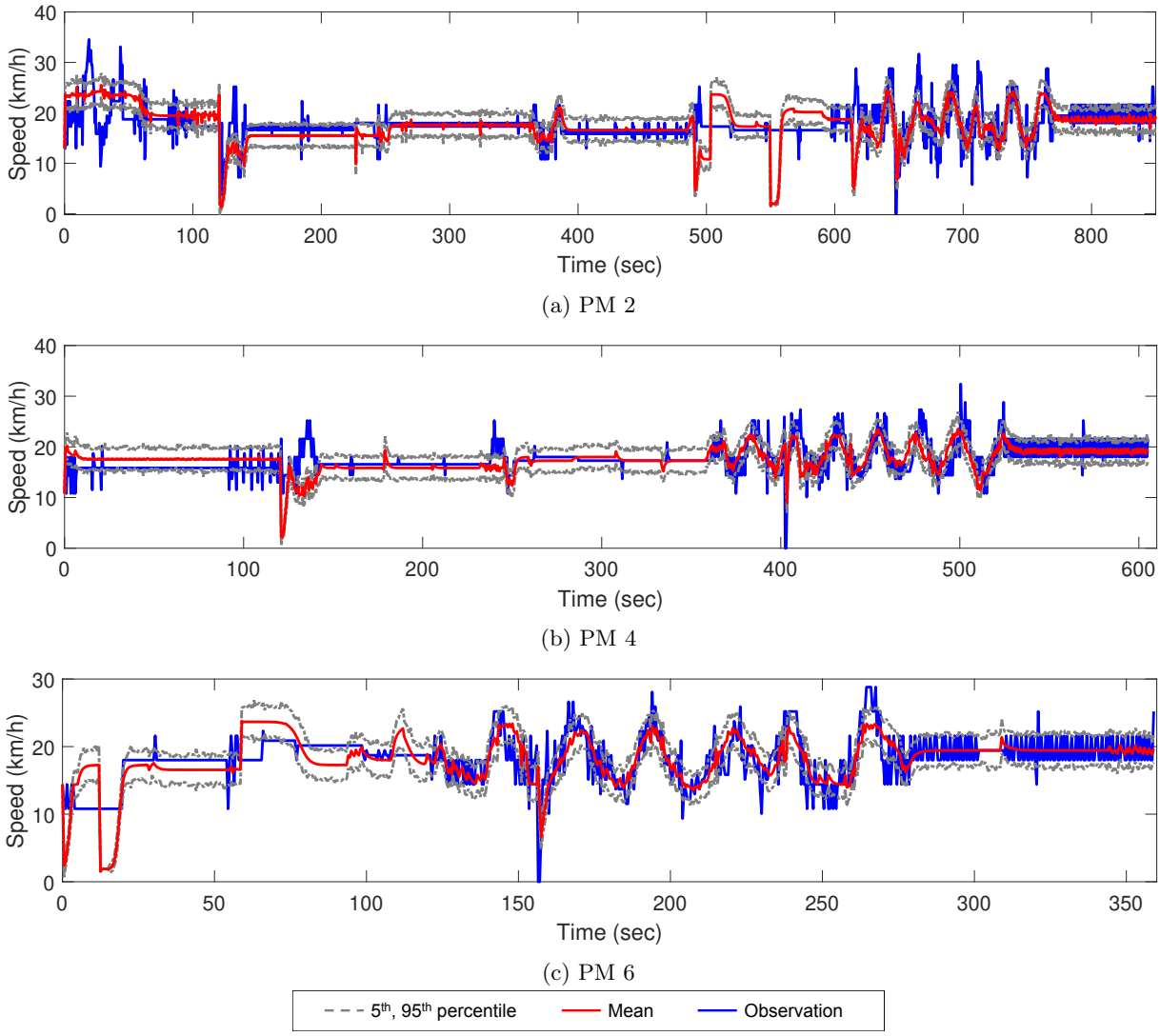

(a) PM 2

(b) PM 4

(c) PM 6

Figure 15: Model validation results of pedestrian-mixed conditions

In Fig. 15, the main streams of observed speed profiles of PM 2, 4, and 6 are well captured by the proposed model, providing mean speed values with the upper and lower stochastic bounds in the validation sets. In the meantime, extremely high or low-speed regimes and initial fluctuations in speed profiles are not fully illustrated by model 5. In addition to the comparisons of speed profiles, we illustrate aggregated space headway to validate excellent performance of the proposed model 5 in Fig. 16. The mean values of all moving trajectories estimated by model 5 are illustrated with observed moving trajectories of all PM riders under the pedestrian-mixed scenario. Red and blue solid lines denote the moving trajectories estimated by model 5 and the observed moving trajectories, respectively.

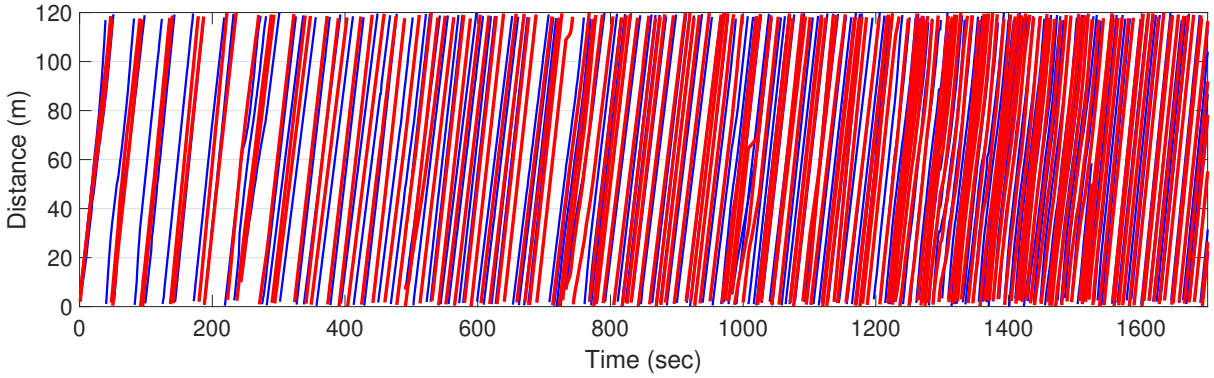

(a) Trajectories during a whole analysis period

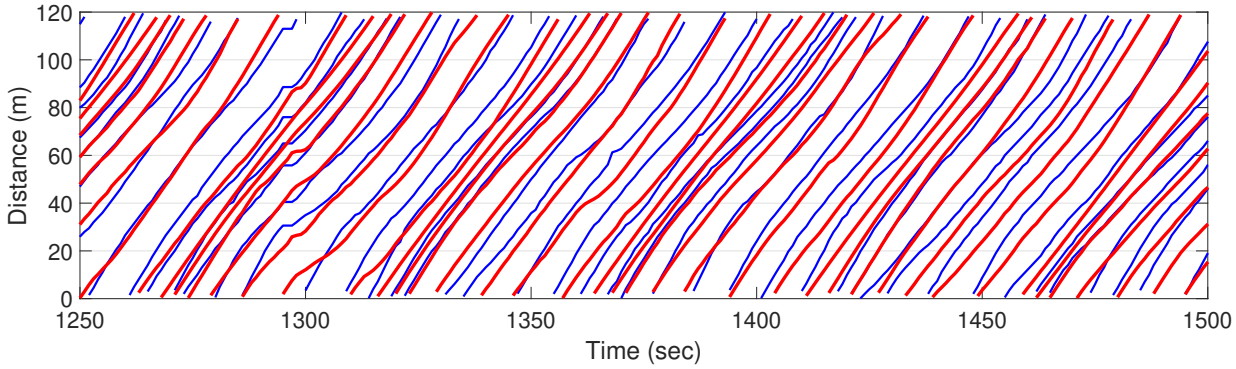

(b) Trajectories from 1250s to 1500s

Figure 16: the observed and the estimated moving trajectories under pedestrian-mixed flow

In Fig. 16a, the overall spacing behaviour of PM devices is well described by the proposed model in validation sets under pedestrian-mixed flow conditions. Moreover, the proposed SFVDM captures the spacing behaviour of PM riders newly joined or left, the leading riders, and the following riders at around 500s, 1000s, and 1500s. In Fig. 16b, model 5 describes primary streams of spacing behaviour of all PM devices in the enlarged period from 1250s to 1500s, which is the highest density period. In the meantime, sudden acceleration and deceleration manoeuvres of PM riders around 1300s are not fully captured by the proposed model in the validation process.

In Fig. 11b, the proposed model illustrates the spacing behaviour of PM devices, which is similar to the observed spacing trajectories from 500s to 750s, which is one of the highest density periods, whereas, the tiny fluctuations in the spacing profiles are not fully covered by the proposed model under pedestrian-mixed conditions.

6.3. PMs behaviour in low-speed homogeneous conditions

To take account of stochastic behaviour characteristics of PM devices under low-speed homogeneous traffic conditions, we calibrate only two models, which have different sets of parameters depending on the base model, in the following table. Meanwhile, we exclude two models, containing anticipation factors, due to homogeneous conditions. After comparisons of performance between models, we validate model 5 based on unused data set in the calibration process under low-speed conditions.

6.3.1. Model calibration

The parameters are mean values in the case of individual calibration processes. Table 12 includes mean values and standard deviations of parameters calibrated in behaviour models of individual PM devices to describe the heterogeneity of the parameters among PM riders under low-speed running homogeneous conditions.

Table 12: Calibration results under low-speed homogeneous conditions

		Model 1	Model 2	Model 3	Model 4
δ_2	Mean	n/a	n/a	n/a	n/a
	SD	n/a	n/a	n/a	n/a
λ_2	Mean	n/a	n/a	n/a	n/a
	SD	n/a	n/a	n/a	n/a
σ_0	Mean	n/a	0.2455	n/a	n/a
	SD	n/a	0.1902	n/a	n/a
V_0	Mean	n/a	3.5010	n/a	2.3496
	SD	n/a	0.7852	n/a	0.2126
C	Mean	n/a	0.8886	n/a	2.4374
	SD	n/a	0.3714	n/a	0.7696
b	Mean	n/a	7.1436	n/a	2.9980
	SD	n/a	2.5629	n/a	1.2284
γ	Mean	n/a	1.1491	n/a	0.1000
	SD	n/a	0.1247	n/a	3.50E-05
κ	Mean	n/a	n/a	n/a	0.7540
	SD	n/a	n/a	n/a	0.3070

In Table 12, the mean value of the dissipation coefficient, σ_0, 0.25, with 0.19 of the standard deviation shows that the stochastic PM devices well capture behavioural uncertainty following models under low-speed homogeneous conditions. The average desired speed of PM devices is between 2.3 and 3.5 m/s, which are largely smaller than previous cases of mixed traffic conditions within a boundary of the specification of PM devices in a market. Moreover, their values of standard deviations are 0.8 and 0.2 for Model 2 and Model 4, respectively, in which the value of Model 4 is smaller than heterogeneous traffic conditions. Values of a shape of the equilibrium flow-density relations, C, are 0.89 and 2.4 for Model 2 and Model 4, respectively. Their mean and standard deviations are smaller than their values of heterogeneous traffic conditions in Section 6.2 and Section 6.1. The values of length scale, b, of Model 2 and Model 4 are 7.1 and 3.0, respectively, meanwhile, the space headway coefficients, γ, are between 0.1 and 1.1. Their values of mean and standard deviations are smaller than their values of heterogeneous traffic conditions in Section 6.2 and Section 6.1. The relative speed coefficient, κ, is 0.75, which is between bike-mixed and pedestrian-mixed traffic conditions with 0.3 of similar values of standard deviations. The fitted-trajectories of speed profiles are selected to compare the two models' performance in Table 12 in the following figure.

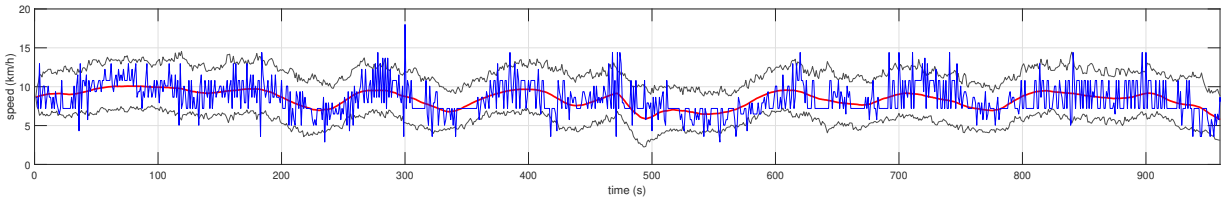

(a) Model 2 with stochasticity

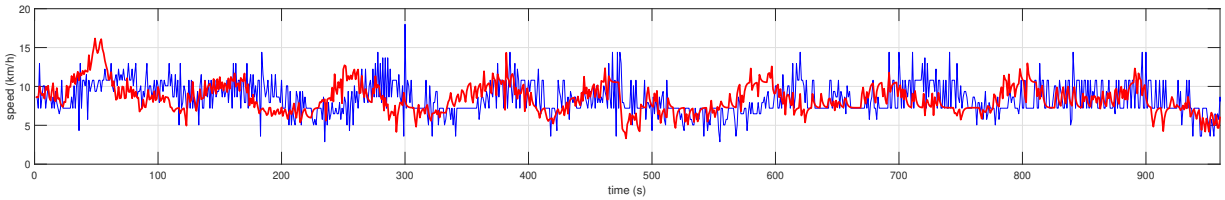

(b) Model 4 with anticipation factors

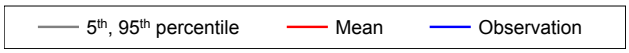

Figure 17: Speed profiles of the top two models in the second PM device under low-speed homogeneous flow conditions

In Fig. 17a, the model 2 explains the main fluctuations in the speed of the following PM device within the upper and lower boundary of speed profiles, although the calibrated speed profiles miss the finest fluctuations in the real speed profiles. In Fig. 17b, model 4 captures fine fluctuations in PM speed profiles, whereas it does not contain all of the main streams in the real speed profiles.

After comparing the top two models' performance, we calibrate model 5, the results of which are given in the following tables and figures.

Table 13: Calibration results of the proposed model 5 under low-speed traffic conditions

	δ_2	λ_2	σ_0	V_0	C	b	γ	κ
Model 5	n/a	n/a	0.1648	2.8805	1.6876	8.5964	0.1747	0.0195

In Table 13, the value of positive dissipation parameters, σ_0, 0.1648, shows that behavioural uncertainty is well captured by the stochastic PM devices following models under mixed traffic conditions. The average desired speed of PM devices is 2.9 m/s, which is within the specification of PM devices in a market. Other calibrated variables of the finally proposed model 5 are slightly different from the previous models. The statistics of calibration results are illustrated in the following table.

Table 14: Values of final value of GA of the models under low-speed traffic conditions

	Model 1	Model 2	Model 3	Model 4	Model 5
Final value of GA	n/a	2.1431	n/a	3.0491	1.6717
Improvement than the base model	n/a	n/a	n/a	-42.28%	22.00%

In Table 14, models 2 and 5 show better performance than model 4. It implies that stochastic behavioural models of PM devices against homogeneous traffic conditions greatly influence the improvement of model performance than considering relative speed under homogeneous low-speed PM conditions. The calibrated results are described in the following figures.

In Fig. 18, the SFVDM based behaviour model of PM devices illustrates main speed tendency and tiny fluctuations in speed within the lower and upper bound of PM speed. It also captures the unstable

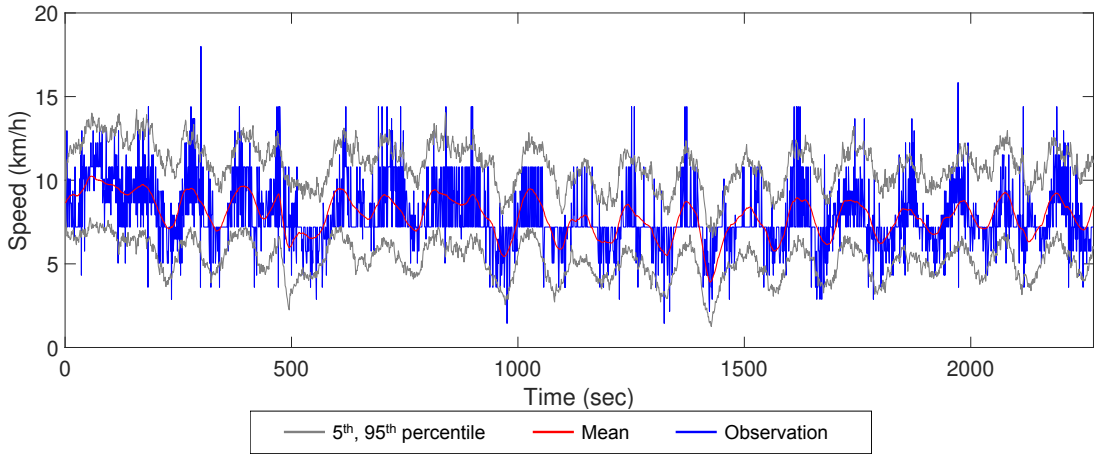

Figure 18: Performance of stochastic FVDM-based behaviour models of the second PM devices under low-speed homogeneous flow conditions

behaviour at very low speed. This conforms to the low-speed regime's instabilities due to the stochastic factor, as explained in Ngoduy et al. (2019).

6.3.2. Model validation

Trajectories of PM devices 1, 3, 5, and 7 are used to globally calibrate model 5, including the stochastic force and two anticipation factors in the form of SFVDM. Those devices 2, 4, and 6 are used for model validation under low-speed homogeneous conditions. The global calibration results of model 5 are illustrated in Table 15.

Table 15: Global calibration results of model 5 under low-speed traffic conditions

	δ_2	λ_2	σ_0	V_0	C	b	γ	κ
Model 5	n/a	n/a	0.3722	2.7410	2.2699	3.6036	0.6250	0.0181

The globally calibrated parameters in Table 15 are slightly different from the parameters calibrated by trajectories of PM 2 only in Table 13 due to its diversity in the calibration set. The calibrated mean values of speed of PM 1, 3, 5, and 7 are provided with the upper (95 percentile of confidence interval) and lower (5 percentile of confidence interval) bound in Fig. 19. They are compared with the ground truth speed profiles of each corresponding PM device.

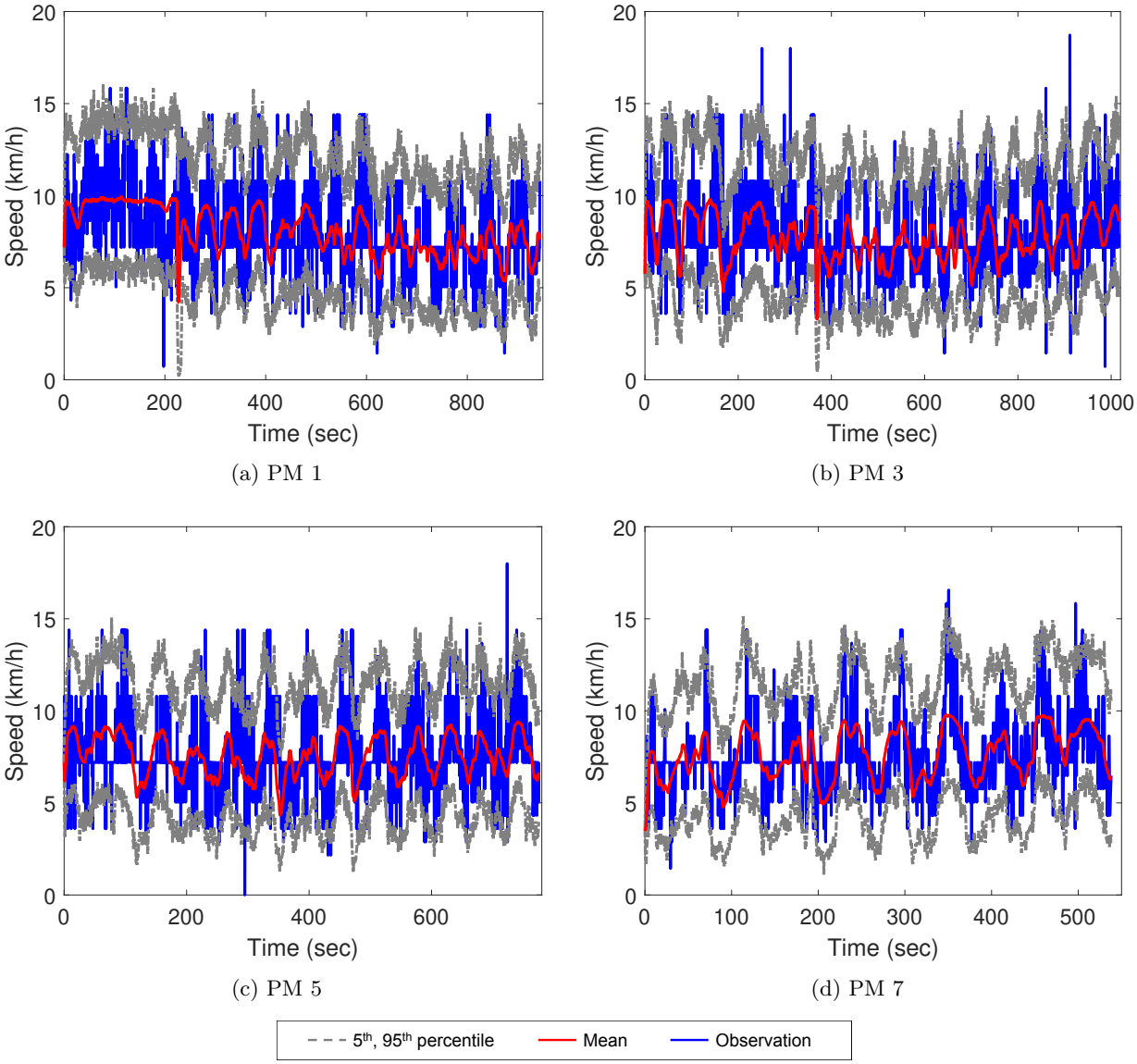

Figure 19: Global calibration results in low-speed traffic conditions

In Fig. 19, the ground truth speed profiles of PM devices are within the upper and the lower stochastic bound of the estimated mean speed. We validate the calibrated SFVDM with the ground truth speed profiles of PM devices 2, 4, and 6 in Fig. 20.

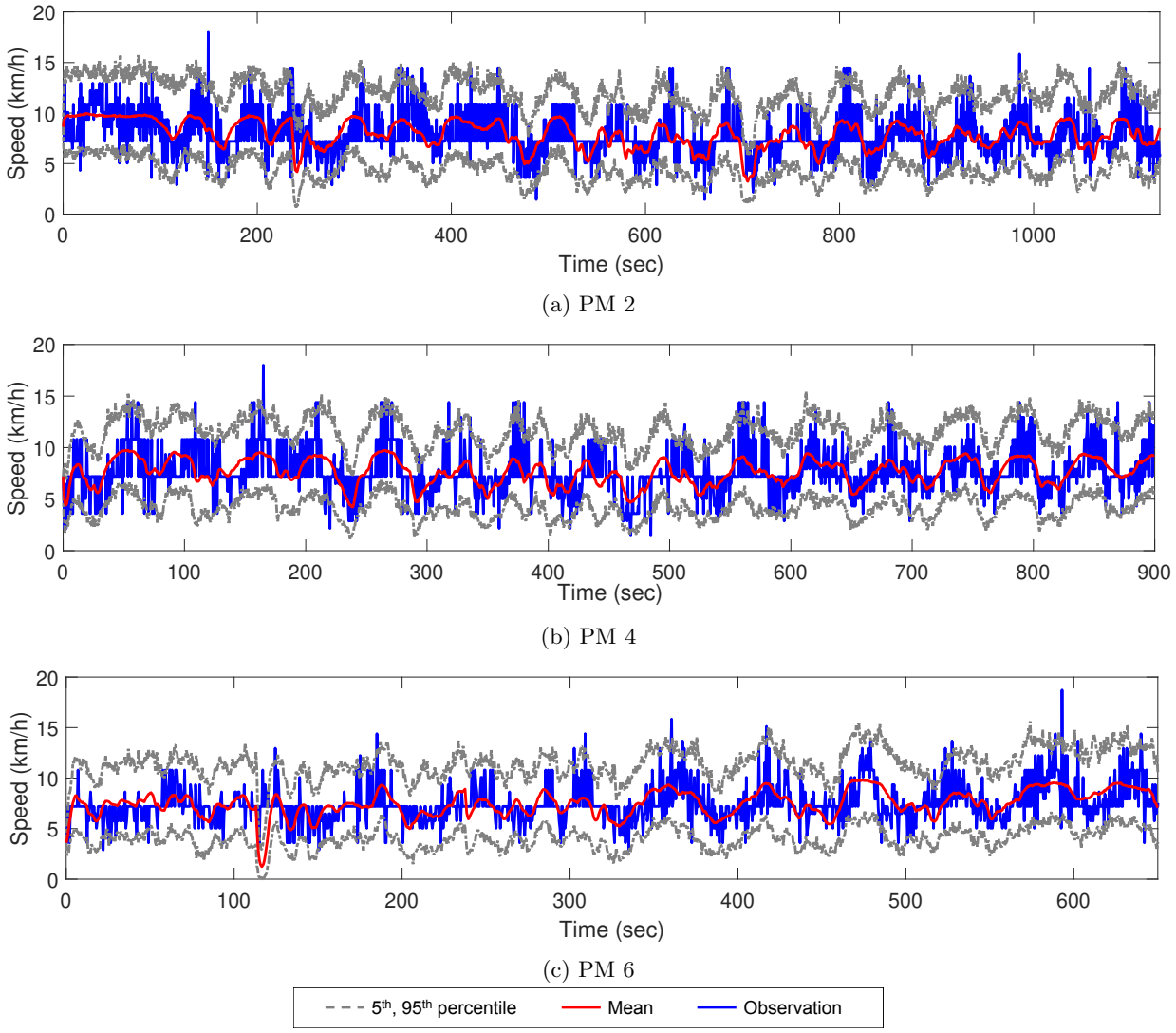

Figure 20: Model validation results of low-speed traffic conditions

In Fig. 20, the observed speed profiles of PM devices are within the upper and the lower stochastic bounds under low-speed traffic conditions in the validation sets. In addition to the comparisons of speed profiles, we illustrate aggregated space headway to validate excellent performance of the proposed model 5 in Fig. 21. The mean values of all moving trajectories estimated by model 5 are illustrated with observed moving trajectories of all PM riders under the low-speed traffic flow scenario. Red and blue solid lines denote the moving trajectories estimated by model 5 and the observed moving trajectories, respectively.

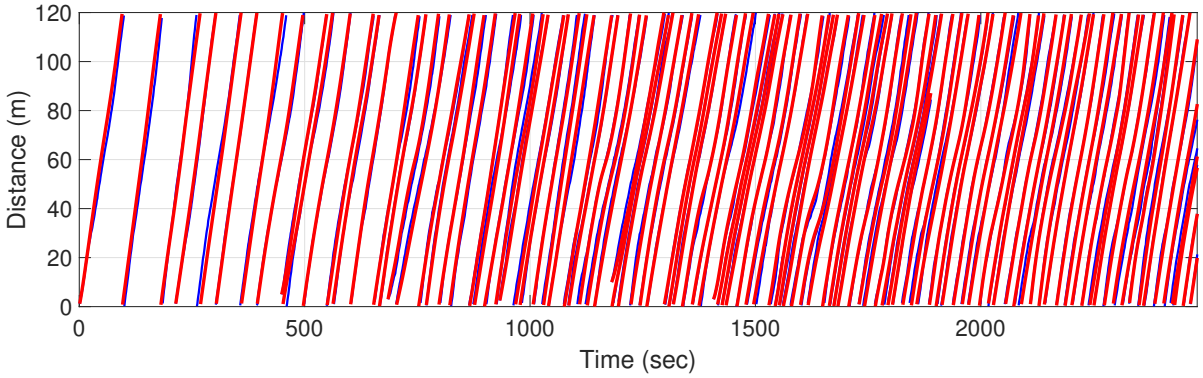

(a) Trajectories during a whole analysis period

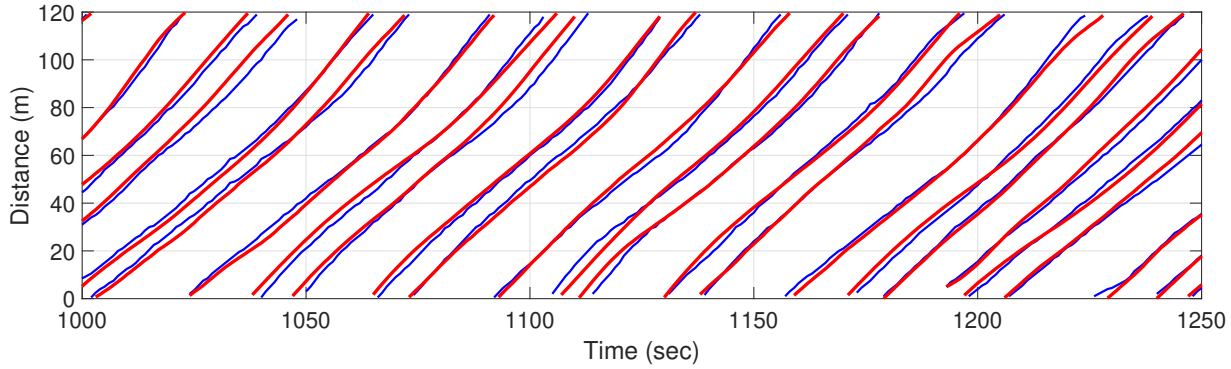

(b) Trajectories from 1000s to 1250s

Figure 21: the observed and the estimated moving trajectories under low-speed flow

In Fig. 21a, the comprehensive spacing behaviour of PM devices is well described by the proposed model under homogeneous low-speed traffic conditions. Moreover, the proposed SFVDM captures the spacing behaviour of PM riders newly joined or left, the leading riders, and the following riders at around 1100s, 1400s, and 1800s. In Fig. 21b, the proposed model shows excellent performance in explaining the spacing behaviour of PM devices in the enlarged period from 1000s to 1250s, which is one of the most congested periods.

6.4. PMs behaviour in high-speed homogeneous conditions

Stochastic behavioural models of PM devices are constructed under high-speed homogeneous traffic conditions, we calibrate only two models, which have different sets of parameters depending on the base model, in the following table. Meanwhile, we exclude two models, containing anticipation factors, due to homogeneous conditions. After comparisons of performance between models, we validate model 5 based on unused data set in the calibration process under high-speed conditions.

6.4.1. Model calibration

The parameters are mean values in the case of individual calibration processes. Table 12 contains calibration results of Models 1 to 4 under high-speed running homogeneous traffic conditions. Mean values and standard deviations are provided for parameters calibrated in behaviour models of individual PM devices to describe the heterogeneity of the parameters among PM riders under high-speed running homogeneous conditions.

Table 16: Calibration results under high-speed homogeneous conditions

		Model 1	Model 2	Model 3	Model 4
δ_2	Mean	n/a	n/a	n/a	n/a
	SD	n/a	n/a	n/a	n/a
λ_2	Mean	n/a	n/a	n/a	n/a
	SD	n/a	n/a	n/a	n/a
σ_0	Mean	n/a	0.1448	n/a	n/a
	SD	n/a	0.1008	n/a	n/a
V_0	Mean	n/a	6.6280	n/a	4.0126
	SD	n/a	0.5629	n/a	0.4579
C	Mean	n/a	1.3298	n/a	1.5160
	SD	n/a	0.4112	n/a	0.6532
b	Mean	n/a	7.6634	n/a	2.5587
	SD	n/a	1.8695	n/a	0.8116
γ	Mean	n/a	1.1243	n/a	0.1000
	SD	n/a	0.6306	n/a	1.39E-10
κ	Mean	n/a	n/a	n/a	0.8991
	SD	n/a	n/a	n/a	0.2472

In Table 16, the value of the positive dissipation parameter, σ_0, 0.14, with 0.1 of standard deviation shows that behavioural uncertainty is well captured by the stochastic PM devices following models under high-speed homogeneous conditions. The average desired speed of PM devices is between 4.0 and 7.0 m/s, which are larger than previous all cases, due to the physical specification of PM devices, with similar values of standard deviations to low-speed running conditions. A shape of the equilibrium flow-density relations, C, of Model 2 and Model 3 is stable with 1.3 and 1.5 of mean values and 0.4 and 0.6 of standard deviations, respectively, meanwhile, the values of the length scale of two models are largely different as 7.6 and 2.5 of mean values and 1.8 and 0.8 of standard deviations, respectively. Furthermore, the space headway coefficients, γ, of Model 2 and Model 4 are 1.1 and 0.1 with 0.6 and 0.0 of standard deviations, respectively. Values of γ in Model 4 calibrated in individual trajectories of all PM devices are bounded on the lower limit of values. Whereas the relative speed coefficient, κ, is very significant as 0.90 of mean values and 0.2 of standard deviations. The fitted-trajectories of speed profiles are selected to compare the two models' performance in Table 16 in the following figure.

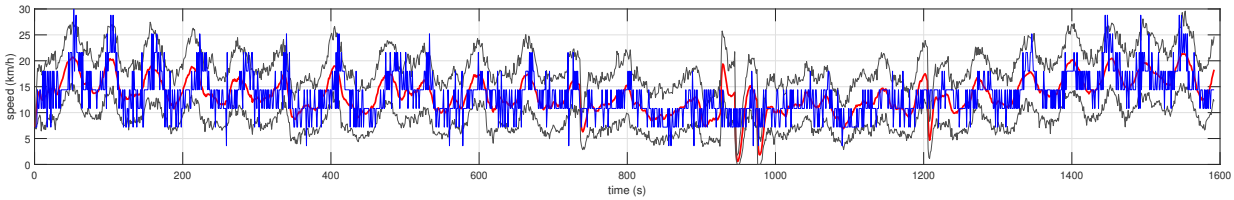

(a) Model 2 with stochasticity

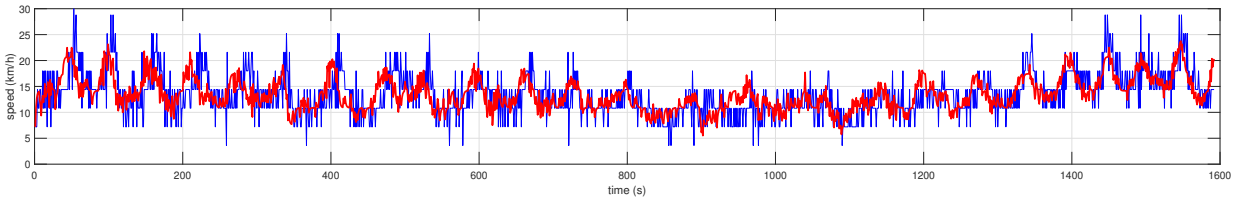

(b) Model 4 with anticipation factors

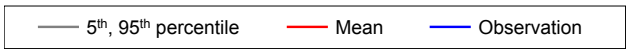

Figure 22: Speed profiles of the top two models in the third PM device under high-speed homogeneous flow conditions

In Fig. 22a, model 2 explains the main fluctuations in the speed of the following PM device within the upper and lower boundary of speed profiles, meanwhile, model 4 illustrates fine fluctuations in PM speed profiles.

After comparing the performance of the top two models, we calibrate model 5 with results given the following tables and figures.

Table 17: Calibration results of the proposed model 5 under high-speed traffic conditions

	δ_2	λ_2	σ_0	V_0	C	b	γ	κ
Model 5	n/a	n/a	0.028	6.6842	1.3484	7.7435	1.2857	0.0001

In Table 17, the value of positive dissipation parameters, σ_0, 0.028, shows that behavioural uncertainty is not sufficiently captured by the stochastic PM devices following models under mixed traffic conditions. The average desired speed of PM devices is 6.7 m/s, which is within the specification of PM devices in a market. Other calibrated variables of the finally proposed model 5 are slightly different from the previous incomplete models because it considers both relative speed and space headway and follows a form of stochastic differential equations. The statistics of calibration results are illustrated in the following table.

Table 18: Values of final value of GA of the models under high-speed traffic conditions

	Model 1	Model 2	Model 3	Model 4	Model 5
Final value of GA	n/a	4.0839	n/a	4.7219	3.3406
Improvement than the base model	n/a	n/a	n/a	-15.62%	18.20%

In Table 18, models 2 and 5 show better performance than model 4. It implies that stochastic behavioural models of PM devices against homogeneous traffic conditions have a great influence on the improvement of model performance than considering relative speed under homogeneous high-speed PM conditions. The calibrated results are described in the following figures.

In Fig. 23, the SFVDM based behaviour model of PM devices illustrates main speed tendency and tiny fluctuations in speed within small lower and upper bound of PM speed. This implies that SFVDM can

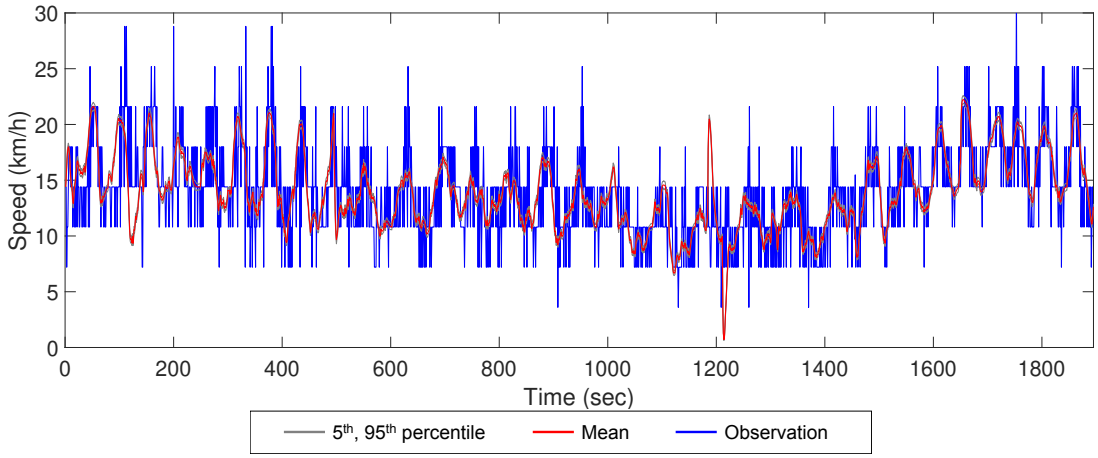

Figure 23: Performance of stochastic FVDM-based behaviour models of the second PM devices under high-speed homogeneous flow conditions

tackle the stochastic behaviour of the following PM device under low-speed homogeneous conditions.

6.4.2. Model validation

Trajectories of PM devices 1, 3, 5, and 7 are used to globally calibrate model 5, which includes the stochastic force and two anticipation factors in the form of SFVDM. Those devices 2, 4, and 6 are used for model validation under high-speed homogeneous conditions. The global calibration results of model 5 are illustrated in Table 19.

Table 19: Global calibration results of model 5 under high-speed traffic conditions

	δ_2	λ_2	σ_0	V_0	C	b	γ	κ
Model 5	n/a	n/a	0.3945	6.8648	2.5329	4.5411	0.2038	0.2212

The globally calibrated parameters in Table 19 are different from the parameters calibrated by trajectories of PM 2 only in Table 17 due to its diversity in the data set. The calibrated mean values of speed of PM 1, 3, 5, and 7 are provided with the upper (95 percentile of confidence interval) and lower (5 percentile of confidence interval) bound in Fig. 24. They are compared with the ground truth speed profiles of each corresponding PM device.

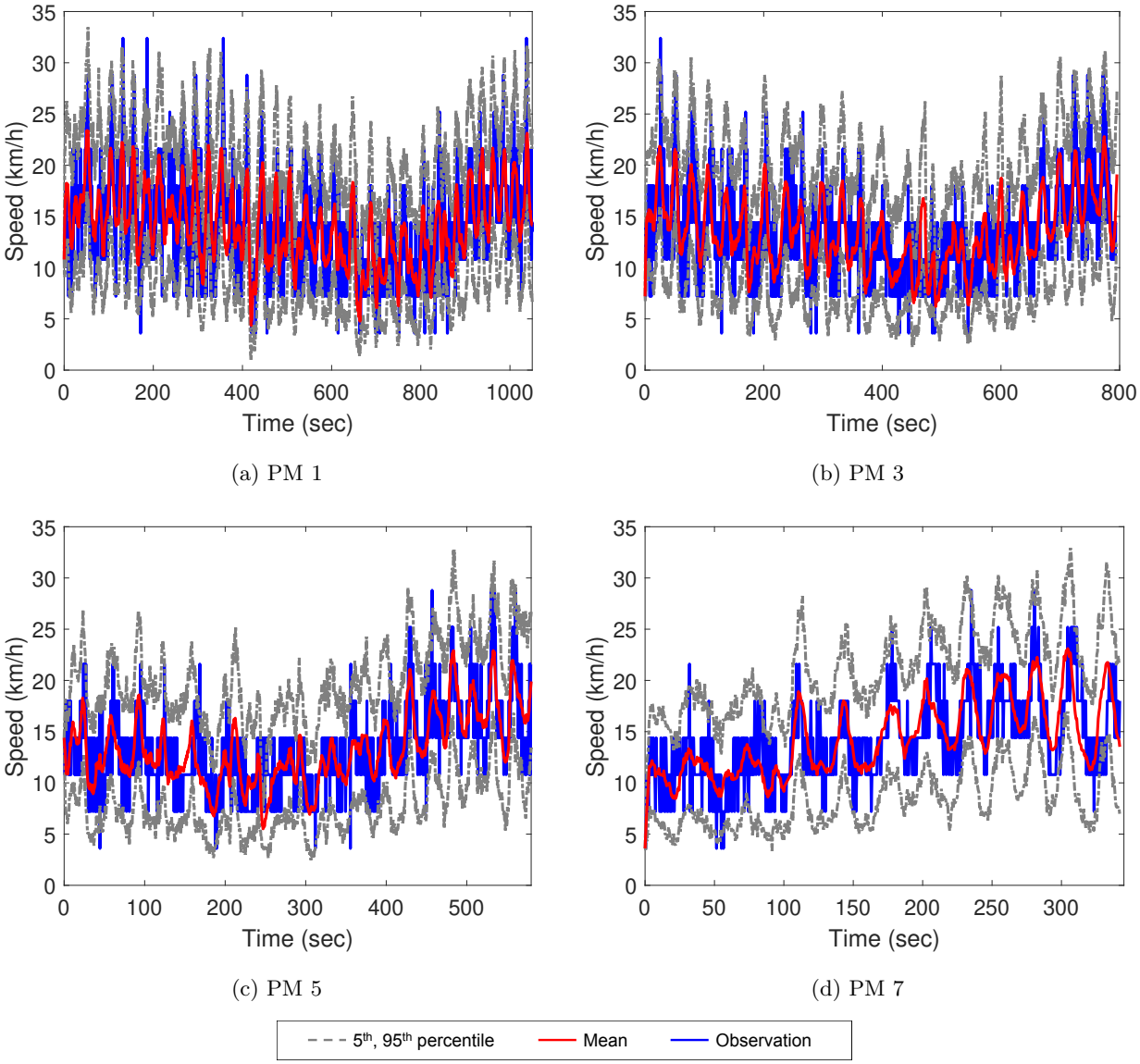

(a) PM 1

(b) PM 3

(c) PM 5

(d) PM 7

Figure 24: Global calibration results in high-speed traffic conditions

In Fig. 24, the ground truth speed profiles of PM devices are within the upper and the lower stochastic bound of the estimated mean speed. We validate the calibrated SFVDM with the ground truth speed profiles of PM devices 2, 4, and 6 in Fig. 25.

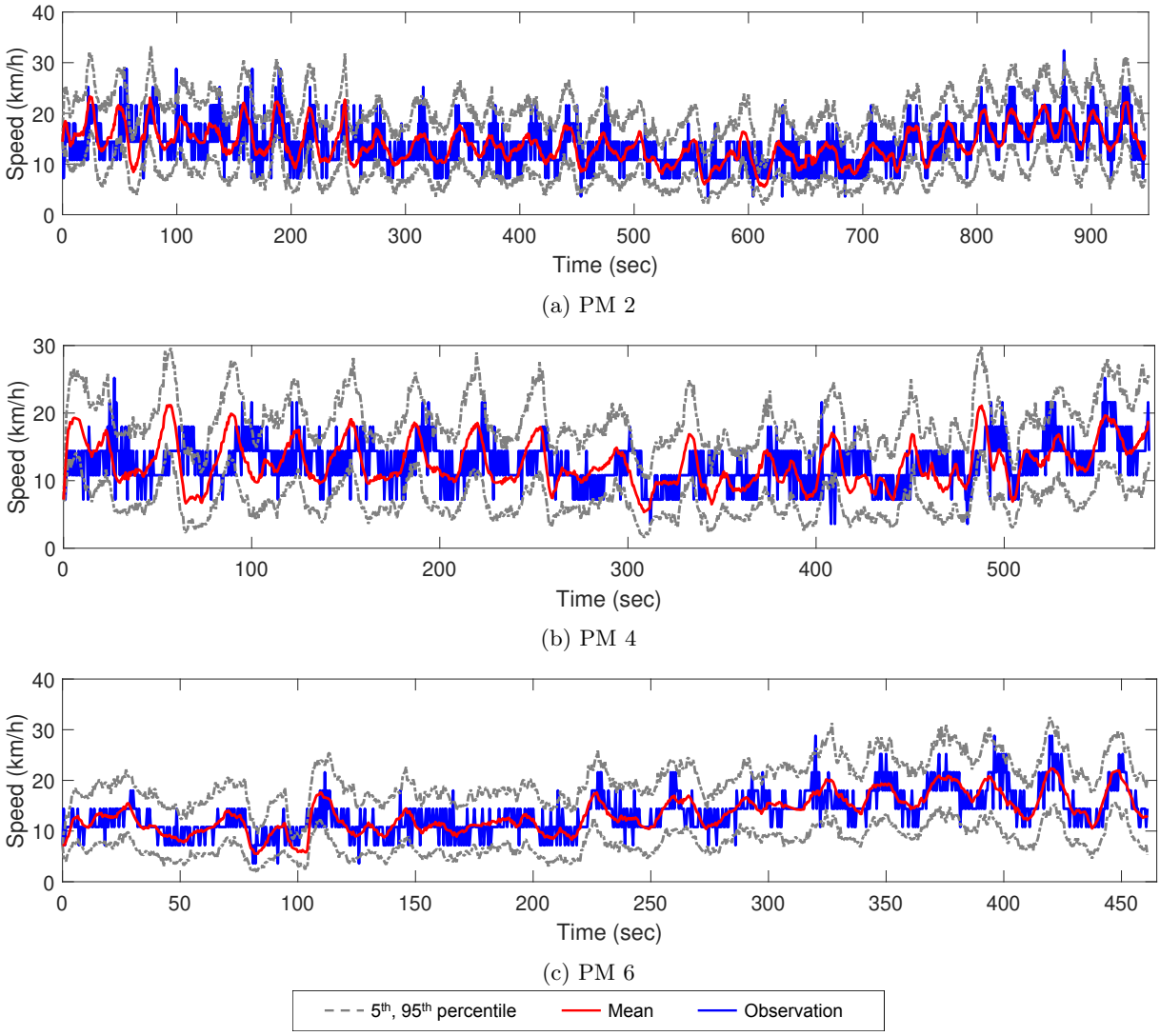

(a) PM 2

(b) PM 4

(c) PM 6

Figure 25: Model validation results of high-speed traffic conditions

In Fig. 25, primary streams and tiny fluctuations in speed profiles of PM 2, 4, and 6 are within the upper and lower 5 percentiles of estimated mean speed by model 5. In addition to the comparisons of speed profiles, we illustrate aggregated space headway to validate excellent performance of the proposed model 5 in Fig. 26. The mean values of all moving trajectories estimated by model 5 are illustrated with observed moving trajectories of all PM riders under the high-speed traffic flow scenario. Red and blue solid lines denote the moving trajectories estimated by model 5 and the observed moving trajectories, respectively.

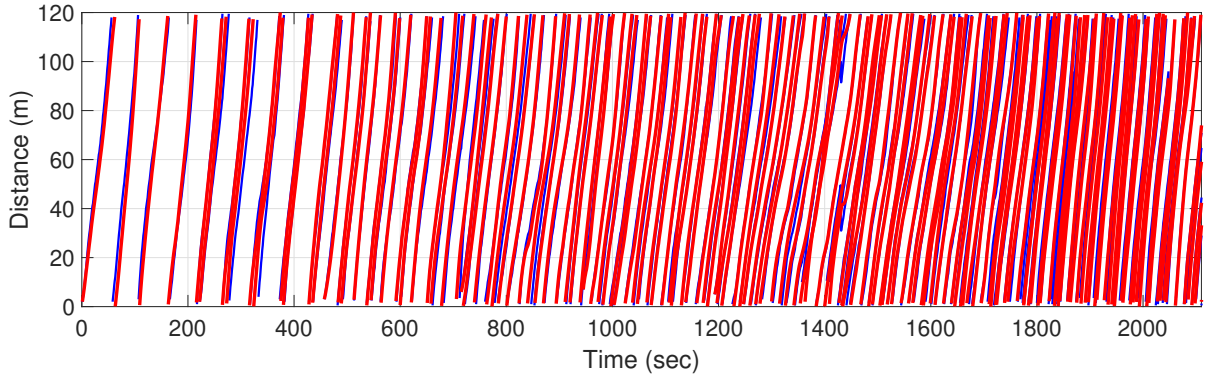

(a) Trajectories during a whole analysis period

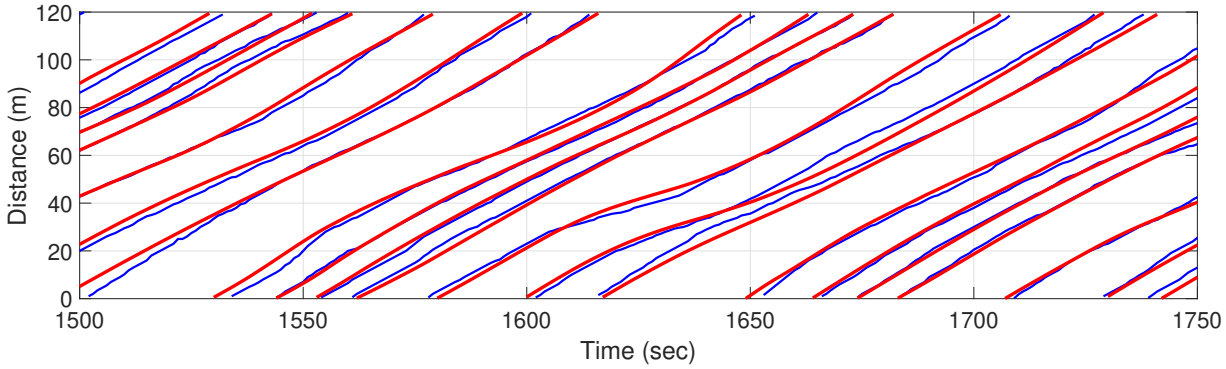

(b) Trajectories from 1500s to 1750s

Figure 26: the observed and the estimated moving trajectories under high-speed flow

In Fig. 26a, model 5 well explains the overall spacing behaviour of all PM devices under homogeneous high-speed flow conditions for the whole analysis period. Moreover, the proposed SFVDM captures spacing behaviour of PM riders newly joined or left, the leading riders, and the following riders at around 700s, 900s, 1200s, and 2000s. In the meantime, the estimates are in discord with the observations when the observation has errors at 40m and 100m at around 1400s. In Fig. 26b, the proposed model shows good performance in estimating the spacing behaviour of PM devices in the enlarged period from 1500s to 1750s, which is one of the most congested periods.

6.5. Discussion

To find the best model of PMs behaviour under diverse traffic conditions, five different behaviour models of PM devices were compared under different driving conditions, including bike-mixed, pedestrian-mixed, low-speed running, and high-speed running conditions, in Section 6.1, Section 6.2, Section 6.3, and Section 6.4. Seven PM devices joined the running stream based on gap acceptance abilities under four different initial scenarios. Trajectories of seven PM devices are used to calibrate five models via the Genetic algorithm locally, and then, the calibration results are given in corresponding sections. Stochasticity through the Langevin force is applied in model 1, model 2, and model 5 throughout experiments. Moreover, the relative speed is adopted as a form of FVDM in model 3, model 4, and model 5 under four different traffic conditions. In model 1, model 3, and model 5, anticipation factors are used to measure the effect on the following PM devices from space headway and relative speed against the heterogeneous leading modes in a shared lane.

Model 1 and model 2 performed better under pedestrian-mixed traffic conditions rather than bike-mixed traffic conditions. In these models, constant sensitivity coefficients played an essential role in improving model performance with lower standard deviation in the pedestrian-mixed case than the bike-mixed case without considering relative speed. Moreover, model 2 showed better performance than model 1 in cases of pedestrian-mixed conditions due to the introduction of anticipation factors to speed of the follower against a device, whereas these factors do not have a significant influence on behavioural modelling of PM devices under bike-mixed conditions. Model 3 and 4 performed very similarly under bike-mixed and pedestrian-mixed traffic conditions since anticipation factors are not significantly working in the model without considering stochastic characteristics of the behaviour of PM devices. In the meantime, their performance is highly better than model 1 and 2 due to introducing the constant sensitivity coefficient of the relative speed under mixed traffic conditions. Excellent performance of model 5 implies that anticipation factors and stochasticity created by the Langevin formula have a synergy influence on behavioural modelling of PM devices under heterogeneous flow conditions. Under homogeneous traffic conditions, model 4 does not show better performance than model 2 even though it includes the constant sensitivity coefficient of the relative speed. From the calibrated results, the constant sensitivity coefficient of the optimal speed and the relative speed countervailed their influence on behavioural modelling of PM devices under low- and high-speed running PM flow conditions. The sensitivity coefficients of the relative speed in model 4 are significantly different between low-speed and high-speed running conditions. The optimal speed is bounded at lower limits of parameters across all PM devices under both conditions. In the meantime, simultaneously considering stochasticity, relative speed, and anticipation factors have a positive influence on the improvement of model performance in model 5 under both heterogeneous and homogeneous traffic conditions. It reduced redundant stochastic upper and lower boundaries of the behaviour following models of PM devices and tackled main streams and tiny fluctuations in speed profiles of PM devices under diverse traffic conditions.

To verify the excellent performance of model 5, SFVDM, we globally calibrate the model using trajectories of PM devices 1, 3, 5, and 7 and then, validate the model using PM 2, 4, and 6. The stochastic and anticipation parameters are calibrated through global model calibrations under each different flow condition. The calibrated model 5 shows reliable performance in the validation set. The overall streams of spacing behaviour of PM devices are fully captured by model 5 under four different conditions, meanwhile, the tiny fluctuations in spacing behaviour caused by sudden acceleration and deceleration manoeuvres are not partially explained by model 5. Consequently, we confirmed that the stochastic force, anticipation factors, and relative speed significantly influenced PM devices' behaviour under hetero- and homogeneous traffic conditions in a single shared lane.

7. Concluding remarks

We have constructed a stochastic behavioural model of PM devices under heterogeneous traffic conditions to cope with spatiotemporal interactions between different green transport modes in a single shared lane. This study provides the novel approach to explain stochastic characteristics of a personal mobility in a single shared lane through the mature-theoretical framework, the vehicular CF model. Anticipation factors are newly introduced in the proposed PM behavioural model to tackle unpredictable fluctuations in the velocity of PM devices against relative speed and space headway to surrounding low-carbon modes under heterogeneous traffic conditions. Moreover, stochastic volatility derived from interactions between intra- and inter-sustainable modes, which is not captured by the deterministic force, is explained by the Langevin force in the proposed behavioural model of PM devices.

We designed real-world circular experiments to validate the proposed model's performance with anticipation factors under mixed-traffic conditions. We examined the effectiveness of the model components, involving anticipation factors to heterogeneous space headway and relative speed and stochasticity, in the proposed framework under four different traffic conditions in a single shared lane. The finally proposed SFVDM-based behaviour model of PM devices illustrates not only the main streams of speed but also tiny fluctuations in speed within the lower and upper bound of PM speed, although it requires more parameters than the deterministic PM behavioural models. Furthermore, newly created anticipation factors against

space headway and relative speed to heterogeneous modes play a significant role in SFVDM to tackle partial influence on the behaviour of the following PM devices from the leading two different sustainable modes.

The proposed method paves the way for the stochastic CF model's applicability to describe PM devices' behavioural dynamics under mixed traffic conditions using anticipation factors. In addition, it lays the foundation stone of dynamics of PM devices in a shared lane to construct effective regulations and safety standards. The proposed methodology will enable to appraise and design traffic safety facilities for a shared lane through traffic micro-simulation programs, including the newly proposed PM behaviour models with pedestrian and bicycle behaviour models. For future research directions, the proposed model will involve lateral components of interactions to tackle frequent overtaking behaviour of inter- and intra-modes in wider pathways to improve model performance under bike-mixed traffic conditions. We will introduce delayed responses to capture physical oscillations of PM devices under mixed traffic conditions. Besides, the applicability of the proposed stochastic behaviour models of PM devices will be studied to form the platoon of sustainable transport modes under heterogeneous flow conditions.

Acknowledgements

This research was supported by the Basic Science Research Program through the National Research Foundation of Korea (NRF) funded by the Ministry of Education(No. 2018R1D1A1B07051354). This support is gratefully acknowledged.

References

Antonini, G., Bierlaire, M., & Weber, M. (2006). Discrete choice models of pedestrian walking behavior. *Transportation Research Part B: Methodological*, *40*, 667–687.

Asano, M., Iryo, T., & Kuwahara, M. (2010). Microscopic pedestrian simulation model combined with a tactical model for route choice behaviour. *Transportation Research Part C: Emerging Technologies*, *18*, 842–855.

Bando, M., Hasebe, K., Nakanishi, K., & Nakayama, A. (1998). Analysis of optimal velocity model with explicit delay. *Physical Review E*, *58*, 5429.

Bando, M., Hasebe, K., Nakayama, A., Shibata, A., & Sugiyama, Y. (1995). Dynamical model of traffic congestion and numerical simulation. *Physical review E*, *51*, 1035.

BITRE (2015). *Traffic and congestion cost trends for Australian capital cities*. Technical Report Bureau of Infrastructure Transport and Regional Economics Canberra.

Bradley, M. (2018). *Road congestion in Australia*. Technical Report Australian Automobile Association Canberra.

Chandler, R. E., Herman, R., & Montroll, E. W. (1958). Traffic dynamics: studies in car following. *Operations research*, *6*, 165–184.

Constance, A., & Pavey, M. (2018). *Future Transport Strategy 2056*. Technical Report Transport for New South Wales Sydney.

Cox, J. C., Ingersoll Jr, J. E., & Ross, S. A. (1985). A theory of the term structure of interest rates. In *Econometrica* (pp. 385–407). JSTOR volume 53.

Dias, C., Iryo-Asano, M., Nishiuchi, H., & Todoroki, T. (2018). Calibrating a social force based model for simulating personal mobility vehicles and pedestrian mixed traffic. *Simulation Modelling Practice and Theory*, *87*, 395–411.

Fletcher, P. (2017). *Motor Vehicle Standards (Road Vehicles) Determination 2017*. Technical Report Australian Government Canberra.

Gazis, D. C., Herman, R., & Rothery, R. W. (1961). Nonlinear follow-the-leader models of traffic flow. *Operations research*, *9*, 545–567.

Gipps, P. G. et al. (1981). Behavioral car-following model for computer simulation. *Transport. Res.*, *15*, 105–111.

Gunay, B. (2007). Car following theory with lateral discomfort. *Transportation Research Part B: Methodological*, *41*, 722–735.

Guo, N., Hao, Q.-Y., Jiang, R., Hu, M.-B., & Jia, B. (2016). Uni-and bi-directional pedestrian flow in the view-limited condition: experiments and modeling. *Transportation Research Part C: Emerging Technologies*, *71*, 63–85.

Hasegawa, Y., Dias, C., Iryo-Asano, M., & Nishiuchi, H. (2018). Modeling pedestrians' subjective danger perception toward personal mobility vehicles. *Transportation research part F: traffic psychology and behaviour*, *56*, 256–267.

Heinen, E., Van Wee, B., & Maat, K. (2010). Commuting by bicycle: an overview of the literature. *Transport reviews*, *30*, 59–96.

Helbing, D., & Molnar, P. (1995). Social force model for pedestrian dynamics. *Physical review E*, *51*, 4282.

Helbing, D., & Tilch, B. (1998). Generalized force model of traffic dynamics. *Physical review E*, *58*, 133.

Helly, W. (1959). simulation of bottlenecks in single-lane traffic flow. In *Theory of Traffic Flow Symposium Proceedings* (pp. 207–238).

Herman, R. (1959). Car-following and steady state flow. In *Theory of Traffic Flow Symposium Proceedings* (pp. 1–13).

Hoogendoorn, S., & Daamen, W. (2016). Bicycle headway modeling and its applications. *Transportation research record*, *2587*, 34–40.

Jabari, S. E., & Liu, H. X. (2012). A stochastic model of traffic flow: Theoretical foundations. *Transportation Research Part B*, *46*, 156–174.
Jabari, S. E., & Liu, H. X. (2013). A stochastic model of traffic flow: Gaussian approximation and estimation. *Transportation Research Part B*, *47*, 15–41.
Jia, D., & Ngoduy, D. (2016a). Enhanced cooperative car-following traffic model with the combination of V2V and V2I communication. *Transportation Research Part B*, *90*, 172–191.
Jia, D., & Ngoduy, D. (2016b). Platoon based Cooperative Driving Model with Consideration of Realistic Inter-vehicle Communication. *Transportation Research Part C*, *68*, 245–264.
Jia, D., Ngoduy, D., & Vu, H. (2019). A multiclass microscopic model for heterogeneous platoon with vehicle-to-vehicle communication. *Transportmetrica B*, *7*, 448–472.
Jiang, R., Jin, C., Zhang, H., Huang, Y., Tiang, J., Wang, W., M.B., H., Wang, H., & Jia, B. (2018). Experimental and empirical investigations of traffic instability. *Transportation Research Part C*, *94*, 83–98.
Jiang, R., Wu, Q., & Zhu, Z. (2001). Full velocity difference model for a car-following theory. *Physical Review E*, *64*, 017101.
Jin, S., Wang, D., Tao, P., & Li, P. (2010). Non-lane-based full velocity difference car following model. *Physica A: Statistical Mechanics and Its Applications*, *389*, 4654–4662.
Kesting, A., & Treiber, M. (2008). How Reaction Time, Update Time, and Adaptation Time Influence the Stability of Traffic Flow. *Computer-Aided Civil and Infrastructure Engineering*, *23*, 125–137.
Kneidl, A., Hartmann, D., & Borrmann, A. (2013). A hybrid multi-scale approach for simulation of pedestrian dynamics. *Transportation research part C: emerging technologies*, *37*, 223–237.
Kometani, E. (1959). Dynamic behavior of traffic with a nonlinear spacing-speed relationship. *Theory of Traffic Flow (Proc. of Sym. on TTF (GM))*, (pp. 105–119).
Kurtc, V., & Treiber, M. (2020). Simulating bicycle traffic by the intelligent-driver model-reproducing the traffic-wave characteristics observed in a bicycle-following experiment. *Journal of Traffic and Transportation Engineering (English Edition)*, *7*, 19 – 29.
Laval, J. A., Toth, C. S., & Zhou, Y. (2014). A parsimonious model for the formation of oscillations in car-following models. *Transportation Research Part B: Methodological*, *70*, 228–238.
Lee, S., Ngoduy, D., & Keyvan-Ekbatani, M. (2019). Integrated deep learning and stochastic car-following model for traffic dynamics on multi-lane freeways. *Transportation research part C: emerging technologies*, *106*, 360–377.
Li, Y., Zhang, L., Peeta, S., Pan, H., Zheng, T., Li, Y., & He, X. (2015). Non-lane-discipline-based car-following model considering the effects of two-sided lateral gaps. *Nonlinear Dynamics*, *80*, 227–238.
Lighthill, M. J., & Whitham, G. B. (1955). On kinematic waves ii. a theory of traffic flow on long crowded roads. *Proceedings of the Royal Society of London. Series A. Mathematical and Physical Sciences*, *229*, 317–345.
Metkari, M., Budhkar, A., & Maurya, A. K. (2013). Development of simulation model for heterogeneous traffic with no lane discipline. *Procedia-Social and Behavioral Sciences*, *104*, 360–369.
Mohammed, H., Bigazzi, A. Y., & Sayed, T. (2019). Characterization of bicycle following and overtaking maneuvers on cycling paths. *Transportation research part C: emerging technologies*, *98*, 139–151.
Newell, G. F. (1961). Nonlinear effects in the dynamics of car following. *Operations research*, *9*, 209–229.
Newell, G. F. (2002). A simplified car-following theory: a lower order model. *Transportation Research Part B: Methodological*, *36*, 195–205.
Ngoduy, D. (2013). Analytical studies on the instabilities of heterogeneous intelligent traffic flow. *Communications in Nonlinear Science and Numerical Simulation*, *18*, 2699–2706.
Ngoduy, D. (2015a). Effect of the car-following combinations on the instability of heterogeneous traffic flow. *Transportmetrica Part B: Transport Dynamics*, *3*, 44–58.
Ngoduy, D. (2015b). Linear stability of a generalized multi-anticipative car following model with time delays. *Communications in Nonlinear Science and Numerical Simulation*, *22*, 420–426.
Ngoduy, D., Lee, S., Treiber, M., Keyvan-Ekbatani, M., & Vu, H. (2019). Langevin method for a continuous stochastic car-following model and its stability conditions. *Transportation Research Part C: Emerging Technologies*, *105*, 599–610.
Papadimitriou, E., Yannis, G., & Golias, J. (2009). A critical assessment of pedestrian behaviour models. *Transportation research part F: traffic psychology and behaviour*, *12*, 242–255.
Paulsen, M., Rasmussen, T. K., & Nielsen, O. A. (2019). Fast or forced to follow: A speed heterogeneous approach to congested multi-lane bicycle traffic simulation. *Transportation research part B: methodological*, *127*, 72–98.
Pham, T. Q., Nakagawa, C., Shintani, A., & Ito, T. (2015). Evaluation of the effects of a personal mobility vehicle on multiple pedestrians using personal space. *IEEE Transactions on Intelligent Transportation Systems*, *16*, 2028–2037.
Pipes, L. A. (1953). An operational analysis of traffic dynamics. *Journal of applied physics*, *24*, 274–281.
Ravishankar, K., & Mathew, T. V. (2011). Vehicle-type dependent car-following model for heterogeneous traffic conditions. *Journal of transportation engineering*, *137*, 775–781.
Richards, P. I. (1956). Shock waves on the highway. *Operations research*, *4*, 42–51.
Sugiyama, Y., Fukui, M., Kikuchi, M., Hasebe, K., Nakayama, A., Nishinari, K., Tadaki, S., & Yukawa, S. (2008). Traffic jams without bottlenecks–experimental evidence for the physical mechanism of the formation of a jam. *New Journal of Physics*, *10*, 033001–033007.
Sun, D., Chen, D., Zhao, M., Liu, W., & Zheng, L. (2018). Linear stability and nonlinear analyses of traffic waves for the general nonlinear car-following model with multi-time delays. *Physica A*, *501*, 293–307.
Tian, J., Jiang, R., Jia, B., Gao, Z., & Ma, S. (2016b). Empirical analysis and simulation of the concave growth pattern of traffic oscillations. *Transportation Research Part B*, *93*, 338–354.
Tian, J., Jiang, R., Li, G., Treiber, M., Jia, B., & Zhu, C. (2016a). Improved 2D intelligent driver model in the framework

of three-phase traffic theory simulating synchronized flow and concave growth pattern of traffic oscillations. *Transportation Research Part F*, *41*, 55–65.

Tian, J., Zhang, H., Treiber, M., Jiang, R., Gao, J., & Jia, B. (2019). On the role of speed adaptation and spacing indifference in traffic instability: Evidence from car-following experiments and its stochastic model. *Transportation Research Part B*, *129*, 334–350.

Tordeux, A., & Schadschneider, A. (2016). A stochastic optimal velocity model for pedestrian flow. In *Parallel Processing and Applied Mathematics* (pp. 528–538). Springer.

Treiber, M., Hennecke, A., & Helbing, D. (2000). Congested traffic states in empirical observations and microscopic simulations. *Physical review E*, *62*, 1805.

Treiber, M., & Kesting, A. (2013). Traffic flow dynamics. *Traffic Flow Dynamics: Data, Models and Simulation, Springer-Verlag Berlin Heidelberg*, .

Treiber, M., & Kesting, A. (2018). The intelligent driver model with stochasticity – new insights into traffic flow oscillations. *Transportation Research Part B: Methodological*, *117*, 613 – 623. TRB:ISTTT-22.

Treiber, M., Kesting, A., & Helbing, D. (2005). Delays, inaccuracies and anticipation in microscopic traffic model. *Physica A*, *360*, 71–88.

Treiber, M., Kesting, A., & Helbing, D. (2006). Understanding widely scattered traffic flows, the capacity drop, and platoons as effects of variance-driven time gaps. *Physical review E*, *74*, 016123.

Twaddle, H., Schendzielorz, T., & Fakler, O. (2014). Bicycles in urban areas: Review of existing methods for modeling behavior. *Transportation research record*, *2434*, 140–146.

Uhlenbeck, G. E., & Ornstein, L. S. (1930). On the theory of the brownian motion. *Physical review*, *36*, 823.

Ulrich, K. T. (2005). Estimating the technology frontier for personal electric vehicles. *Transportation research part C: Emerging technologies*, *13*, 448–462.

Xiao, Y., Gao, Z., Jiang, R., Li, X., Qu, Y., & Huang, Q. (2019). Investigation of pedestrian dynamics in circle antipode experiments: Analysis and model evaluation with macroscopic indexes. *Transportation Research Part C: Emerging Technologies*, *103*, 174–193.

Zeng, W., Chen, P., Yu, G., & Wang, Y. (2017). Specification and calibration of a microscopic model for pedestrian dynamic simulation at signalized intersections: A hybrid approach. *Transportation Research Part C: Emerging Technologies*, *80*, 37–70.

Zhao, Y., & Zhang, H. (2017). A unified follow-the-leader model for vehicle, bicycle and pedestrian traffic. *Transportation research part B: methodological*, *105*, 315–327.

Zheng, F., Jabari, S. E., Liu, H. X., & Lin, D. (2018). Traffic state estimation using stochastic lagrangian dynamics. *Transportation Research Part B: Methodological*, *115*, 143–165.

Zheng, F., Liu, C., Liu, X., Jabari, S., & Liu, L. (2020). Analyzing the impact of automated vehicles on uncertainty and stability of the mixed traffic flow. *Transportation Research Part C*, *112*, 203–219.

Zheng, Z. (2014). Recent developments and research needs in modeling lane changing. *Transportation research part B*, *60*, 16–32.

Zhou, M., Qu, X., & Li, X. (2017). A recurrent neural network based microscopic car following model to predict traffic oscillation. *Transportation research part C: emerging technologies*, *84*, 245–264.